Zoosyst. Evol. 97 (1) 2021, 281–306 | DOI 10.3897/zse.97.65280

PENSOFT

MUSEUM FÜR NATURKUNDE BERLIN

Integrative descriptions of two new *Macrobiotus* species (Tardigrada, Eutardigrada, Macrobiotidae) from Mississippi (USA) and Crete (Greece)

Matteo Vecchi[1], Daniel Stec[2]

1 *Department of Biological and Environmental Science, University of Jyvaskyla, PO Box 35, FI-40014 Jyväskylä, Finland*

2 *Department of Invertebrate Evolution, Institute of Zoology and Biomedical Research, Faculty of Biology, Jagiellonian University, Gronostajowa 9, 30-387 Kraków, Poland*

http://zoobank.org/BCA8CCAB-C578-4FEB-B053-F483D53922AD

Corresponding authors: Matteo Vecchi (matteo.m.vecchi@jyu.fi), Daniel Stec (daniel_stec@interia.eu)

Academic editor: Pavel Stoev ♦ **Received** 1 March 2021 ♦ **Accepted** 29 April 2021 ♦ **Published** 19 May 2021

Abstract

In this paper, we describe two new *Macrobiotus* species from Mississippi (USA) and Crete (Greece) by means of integrative taxonomy. Detailed morphological data from light and scanning electron microscopy, as well as molecular data (sequences of four genetic markers: 18S rRNA, 28S rRNA, ITS-2 and COI), are provided in support of the descriptions of the new species. *Macrobiotus annewintersae* **sp. nov.** from Mississippi belongs to the *Macrobiotus persimilis* complex (*Macrobiotus* clade B) and exhibits a unique egg processes morphology, similar only to *Macrobiotus anemone* Meyer, Domingue & Hinton, 2014, but mainly differs from that species by the presence of eyes, granulation on all legs, dentate lunulae on legs IV, and of bubble-like structures within the tentacular arms that are present on the distal portion of the egg processes. *Macrobiotus rybaki* **sp. nov.** from Crete belongs to the *Macrobiotus* clade A and is most similar to *Macrobiotus dariae* Pilato & Bertolani, 2004, *Macrobiotus noemiae* Roszkowska & Kaczmarek, 2019, *Macrobiotus santoroi* Pilato & D'Urso, 1976, and *Macrobiotus serratus* Bertolani, Guidi & Rebecchi, 1996, but differs from them mainly in the morphological details of its egg processes and chorion reticulation, but also by a number of morphometric characters. In light of the specific morphology of the egg processes of *Macrobiotus annewintersae* **sp. nov.** and *Macrobiotus anemone*, that are equipped with tentacular arms instead of proper terminal disc, we also provide an updated definition of the *Macrobiotus persimilis* complex.

Key Words

egg ornamentation, integrative taxonomy, *Macrobiotus persimilis* complex, molecular phylogeny, species delineation, water bears

Introduction

Tardigrades are a phylum of micrometazoans distributed worldwide, that inhabit marine and limno-terrestrial environments (Schill 2019). Currently, there are more than 1300 formally recognised tardigrade species (Guidetti and Bertolani 2005; Degma and Guidetti 2007; Degma et al. 2009–2020). In recent years, the number of tardigrade species described with integrative taxonomy has steadily increased (*e.g.*, Surmacz et al. 2019; Bochnak et al. 2020; Kayastha et al. 2020; Tumanov et al. 2020a, b; Guidetti et al. 2021). The accumulation of data from such integrative studies allows at some point for broader examination of phylogenetic relationships within a larger group of organisms. This was the case for the family Macrobiotidae, one of the most speciose and diverse groups among tardigrades, which was recently extensively revised (Stec et al. 2021) and which is partially in focus in this study.

Faunistic and taxonomic studies on the tardigrades of North America are numerous and both local and continental species lists have been compiled (Meyer 2013; Kaczmarek et al. 2016). It is, however, clear from new species in the USA being described (see for example Nelson et al. 2020a), that we are still far from a complete knowledge of the taxonomic diversity of tardigrades in this country. In particular, the tardigrade fauna in the state

of Mississippi (USA) has been investigated only once by Hinton and Meyer (2009) who reported only 9 species (from 20 samples). In contrast, the tardigrade fauna in the neighbouring states have been more thoroughly investigated and consequently more than 20 species have been recorded for Alabama, Louisiana and Arkansas, and about 100 species in Tennessee (Bartels and Nelson 2007; Meyer 2013; Kaczmarek et al. 2016; Nelson et al. 2020b).

The first information on Greek tardigrades was provided 85 years ago (Marcus 1936), and since then only a couple of studies have been explicitly devoted to assessing the diversity in this country (Durante Pasa and Maucci 1979; Maucci and Durante Pasa 1982). On the island of Crete, 28 species (from more than 150 samples) have been listed based on two sampling campaigns alone (Maucci and Durante Pasa 1982). Taking into consideration recent progress in tardigrade taxonomy and faunistic studies brought about by the integrative approach, it is more than likely that the region exhibits higher species diversity and additional sampling effort may reveal more species (Vuori et al. 2020).

In this paper, we provide descriptions of two new *Macrobiotus* species: *Macrobiotus annewintersae* sp. nov. from Mississippi (USA) and *Macrobiotus rybaki* sp. nov. from Crete (Greece) and show their phylogenetic position within the genus *Macrobiotus*. Detailed morphological and morphometric data were obtained using phase contrast and scanning electron microscopy (PCM and SEM, respectively) supported by DNA sequences for four molecular markers (three nuclear – 18S rRNA, 28S rRNA, and ITS-2 – and one mitochondrial – COI).

Materials and methods

Samples and specimens

A mixed leaf litter sample containing *M. annewintersae* sp. nov. was collected in a garden in a suburban area of Jackson, Mississippi (32°21'05"N, 89°56'30"W; 106 m asl; Jyväskylä University (JYU) sample code S207, Jagellonian University (JAG) sample code US.084), and a moss sample from a rock in a xeric shrubland containing *M. rybaki* sp. nov. was collected in Omalos, Crete (35°15'00"N, 23°49'28"E, 30 m asl; JAG sample code GR.011). The samples were examined for tardigrades using the protocol by Dastych (1980), with modifications described in detail in Stec et al. (2015). Live animals and eggs of *M. annewintersae* sp. nov. were placed into culture. Specimens were reared in plastic Petri dishes according to the protocol by Stec et al. (2015). Tardigrades were fed *ad libitum* with unicellular freshwater algae (*Chlorococcum* sp. and *Chlorella* sp.; 1:1, Sciento, UK) and *Lecane inermis* Bryce, 1892 (Rotifera) and kept at 16C under a 2:22 light:dark photoperiod.

In order to perform the taxonomic analysis, animals and eggs were either extracted from culture (*M. annewintersae* ssp. nov.), or directly from the sample (*M. rybaki* sp. nov.) and split into several groups for specific analyses i.e., morphological analysis in PCM and SEM, as well as DNA sequencing (for details see sections "Material examined" provided below in the results section for each species description).

Microscopy and imaging

Specimens for light microscopy were mounted on microscope slides in a small drop of Hoyer's medium and secured with a cover slip, following protocol by Morek et al. (2016). Slides were examined under an Olympus BX53 light microscope with PCM, associated with an Olympus DP74 digital camera or under a Zeiss Axioscope A2 light microscope associated with a MiniVID digital camera. Immediately after mounting, the specimens were checked under PCM for the presence of males and females in each of the studied populations, as the spermatozoa in testes and vasa deferentia are visible for several hours after mounting (Coughlan and Stec 2019; Coughlan et al. 2019). To obtain clean and extended specimens for SEM analysis, tardigrades were processed according to the protocol by Stec et al. (2015). Specimens were examined under high vacuum in a Versa 3D DualBeam SEM at the ATOMIN facility of the Jagiellonian University, Kraków, Poland or in a Raith e-LINE E-beam SEM at Nanoscience Center of University of Jyväskylä, Jyväskylä, Finland. All figures were assembled in Corel Photo-Paint X6, ver. 16.4.1.1281. For structures that could not be satisfactorily focused in a single light microscope photograph, a stack of 2–6 images were taken with an equidistance of ca. 0.2 µm and assembled manually into a single deep-focus image in Corel Photo-Paint X6.

Morphometrics and morphological nomenclature

All measurements are given in micrometres (µm). Sample size was adjusted following the recommendations by Stec et al. (2016). Structures were measured only if their orientation was suitable. Body length was measured from the anterior extremity to the posterior end of the body, excluding the hind legs. The terminology used to describe oral cavity armature and eggshell morphology follows Michalczyk and Kaczmarek (2003) and Kaczmarek and Michalczyk (2017). Macroplacoid length sequence is given according to Kaczmarek et al. (2014). Buccal tube length and the level of the stylet support insertion point were measured according to Pilato (1981). The *pt* index is the ratio of the length of a given structure to the length of the buccal tube expressed as a ratio (Pilato 1981). Measurements of buccal tube widths, heights of claws and eggs follow Kaczmarek and Michalczyk (2017). Morphometric data were handled using the "Parachela" ver. 1.7 template available from the Tardigrada Register (Michalczyk and Kaczmarek 2013). The raw morphometric data are provided as Suppl. materials 1, 2. Tardigrade taxonomy follows Bertolani et al. (2014) and Stec et al.

(2021). Thorpe´s normalisation was performed with the R software (R Core Team 2020) on the morphometric traits following Bartels et al. (2011) (SM.03).

Additional material

Individuals of *Macrobiotus* aff. *polonicus* (JYU sample code S165; 58°52'42"N, 17°55'60"E; 23 m asl: Nynäshamn, Sweden; lichen growing on rock on a roadside in a coastal area; coll. Sept. 2019 by MV and Sara Calhim) were genotyped for all the four markers and added to the phylogenetic reconstruction to increase the number of species included in the phylogenetic analysis. Photographs of eggs from the type series of *Macrobious anemone* Meyer, Domingue & Hinton, 2014 (slides 9551 and 9552) were kindly provided by Harry A. Meyer (McNeese State University, Louisiana, USA). Photographs of eggs from the type series of *M. dariae* Pilato & Bertolani, 2004 (slides PC45s1 and PC45s3) and *M. serratus* Bertolani, Guidi & Rebecchi, 1996 (slides C1907s17 and C1907s30) from the Bertolani collection were kindly provided by Roberto Guidetti (University of Modena and Reggio Emilia, Italy). Additional photos of the paratypes and eggs of *Macrobiotus andinus* Maucci, 1988 were kindly taken for us by Witold Morek and Piotr Gąsiorek (Jagiellonian University, Poland) from the Maucci collection (Natural History Museum of Verona).

Genotyping

DNA was extracted from individual animals following a *Chelex 100* resin (*BioRad*) extraction method by Casquet et al. (2012) with modifications described in detail in Stec et al. (2020a). Each specimen was mounted in water and examined under a light microscope prior to DNA extraction. We sequenced four DNA fragments, three nuclear (18S rRNA, 28S rRNA, ITS2) and one mitochondrial (COI). All fragments were amplified and sequenced according to the protocols described in Stec et al. (2020a); primers with original references are listed in Table 1. Sequencing products were read with the ABI 3130xl sequencer at the Molecular Ecology Lab, Institute of Environmental Sciences of the Jagiellonian University, Kraków, Poland. Sequences were processed in MEGA7 (Kumar et al. 2016) and submitted to NCBI GenBank (Table 2).

Phylogenetic analysis

The phylogenetic analyses were conducted using concatenated 18S rRNA+28S rRNA+ITS-2+COI sequences from Macrobiotidae, with *Richtersius coronifer* (Richters, 1903) and *Dactylobiotus parthenogeneticus* Bertolani, 1982 as outgroups. GenBank accession numbers of all sequences used in the analysis are listed in Table 2. Only species/populations with at least 3 markers were included in the analysis.

The 18S rRNA, 28S rRNA and ITS-2 sequences were aligned using MAFFT ver. 7 (Katoh et al. 2002; Katoh and Toh 2008) with the G-INS-i method (thread=4, threadtb=5, threadit=0, reorder, adjust direction, any symbol, max iterate=1000, retree 1, global pair input). The COI sequences were aligned according to their amino acid sequences (translated using the invertebrate mitochondrial code) with the MUSCLE algorithm (Edgar 2004) in MEGA7 with default settings (i.e., all gap penalties=0, max iterations=8, clustering method=UPGMB, lambda=24). Alignments were visually inspected and trimmed in MEGA7. Model selection and phylogenetic reconstructions were undertaken using the CIPRES Science Gateway (Miller et al. 2010). Model selection was performed for each alignment partition (6 in total: 18S rRNA, 28S rRNA, ITS-2 and three COI codons) using PartitionFinder2 (Lanfear et al. 2016), partitions and model selection process together with results are contained in Suppl. material 4. Bayesian inference (BI) phylogenetic reconstruction was performed using MrBayes v3.2.6 (Ronquist et al. 2012) without BEAGLE. Two runs (one cold chain and three heated chains each) of 20 million generations were used with a burn-in of 2 million generations, sampling a tree every 1000 generations. Posterior distribution sanity was checked using Tracer v1.7 (Rambaut et al. 2018). The MrBayes input file with the input alignment is available as Suppl. material 5, and the MrBayes output consensus tree is available as Suppl. material 6. The phylogenetic tree was visualised with FigTree v1.4.4 (Rambaut 2007) and the image was edited with Inkscape 0.92.3 (Bah 2011).

Results

Taxonomic account

Phylum: Tardigrada Doyère, 1840

Table 1. Primers with their original references used for amplification of the four DNA fragments sequenced in the study.

DNA marker	Primer name	Primer direction	Primer sequence (5'-3')	Primer source
18S rRNA	18S_Tar_Ff1	forward	AGGCGAAACCGCGAATGGCTC	Stec et al. (2017a)
	18S_Tar_Rr1	reverse	GCCGCAGGCTCCACTCCTGG	
28S rRNA	28S_Eutar_F	forward	ACCCGCTGAACTTAAGCATAT	Gąsiorek et al. (2018)
	28SR0990	reverse	CCTTGGTCCGTGTTTCAAGAC	Mironov et al. (2012)
ITS-2	ITS2_Eutar_Ff	forward	CGTAACGTGAATTGCAGGAC	Stec et al. (2018a)
	ITS2_Eutar_Rr	reverse	TCCTCCGCTTATTGATATGC	
COI	LCO1490-JJ	forward	CHACWAAYCATAAAGATATYGG	Astrin and Stüben (2008)
	HCO2198-JJ	reverse	AWACTTCVGGRTGVCCAAARAATCA	

Table 2. GenBank accession numbers of sequences downloaded from GenBank and used in the present study. Newly generated sequences are bolded.

	18S	28S	COI	ITS2	Reference
Dactylobiotus parthenogeneticus	MT373693	MT373699	MT373803	MT374190	Pogwizd and Stec (2020)
Macrobiotus aff. *pseudohufelandi* PL	MN888373	MN888358	MN888325	MN888345	Stec et al. (2021)
Macrobiotus aff. *pseudohufelandi* ZA	MN888374	MN888359	MN888326	MN888346	Stec et al. (2021)
Macrobiotus aff. *polonicus* SE	MW588026	MW588032	MW593929	MW588020	This study
	MW588027	MW588033	MW593930	MW588021	
Macrobiotus annewintersae sp. nov.	MW588024	MW588030	MW593927	MW588018	This study
	MW588025	MW588031	MW593928	MW588019	
Macrobiotus basiatus	MT498094	MT488397	MT502116	MT505165	Nelson et al. (2020)
Macrobiotus caelestis	MK737073	MK737071	MK737922	MK737072	Coughlan et al. (2019)
Macrobiotus canaricus	MH063925	MH063934	MH057765	MH063928	Stec et al. (2018b)
			MH057766	MH063929	
Macrobiotus cf. *pallarii* FI	MN888366	MN888352	MN888312	MN888343	Stec et al. (2021)
				MN888342	
Macrobiotus cf. *pallarii* ME	MN888365	MN888351	MN888316	MN888335	Stec et al. (2021)
				MN888336	
Macrobiotus cf. *pallarii* PL	MN888367	MN888353	MN888313	MN888341	Stec et al. (2021)
			MN888314		
Macrobiotus cf. *pallarii* US	MN888368	MN888354	MN888315	MN888339	Stec et al. (2021)
				MN888340	
Macrobiotus cf. *recens*	MH063927	MH063936	MH057768	MH063932	Stec et al. (2018b)
			MH057769	MH063933	
Macrobiotus crustulus	MT261912	MT261903	MT260371	MT261907	Stec et al. (2020c)
Macrobiotus engbergi	MN443039	MN443034	MN444824	MN443036	Stec et al. (2020b)
			MN444825	MN443037	
			MN444826		
Macrobiotus glebkai	MW247177	MW247176	MW246134	MW247180	Kiosya et al. (2021)
Macrobiotus hannae	MH063922	MH063924	MH057764	MH063923	Nowak and Stec (2018)
Macrobiotus kamilae	MK737070	MK737064	MK737920	MK737067	Coughlan and Stec (2019)
			MK737921		
Macrobiotus macrocalix	MH063926	MH063935	MH057767	MH063931	Stec et al. (2018b)
Macrobiotus noongaris	MK737069	MK737063	MK737919	MK737065	Coughlan and Stec (2019)
				MK737066	
Macrobiotus papei	MH063881	MH063880	MH057763	MH063921	Stec et al. (2018c)
Macrobiotus paulinae	KT935502	KT935501	KT951668	KT935500	Stec et al. (2015)
Macrobiotus polonicus AT	MN888369	MN888355	MN888317	MN888337	Stec et al. (2021)
			MN888318	MN888338	
			MN888319		
Macrobiotus polonicus SK	MN888370	MN888356	MN888320	MN888332	Stec et al. (2021)
			MN888321	MN888333	
				MN888334	
Macrobiotus polypiformis	KX810008	KX810009	KX810011	KX810010	Roszkowska et al. (2017)
			KX810012		
Macrobiotus porifini	MT241900–MT241901	MT241897–MT241898	MT246659 MT246661		Kuzdrowska et al. (2021)
Macrobiotus rybaki sp. nov.	MW588028	MW588034	MW593931	MW588022	This study
	MW588029	MW588035	MW593932	MW588023	
Macrobiotus scoticus	KY797265	KY797266	KY797267	KY797268	Stec et al. (2017b)
Macrobiotus shonaicus	MG757132	MG757133	MG757136	MG757134	Stec et al. (2018d)
			MG757137	MG757135	
Macrobiotus sottilei	MW247178	MW247175	MW246133	MW247179	Kiosya et al. (2021)
Macrobiotus vladimiri	MN888375	MN888360	MN888327	MN888347	Stec et al. (2021)
Macrobiotus wandae	MN435112	MN435116	MN482684	MN435120	Kayastha et al. (2020a)
Mesobiotus harmsworthi	MH197146	MH197264	MH195150	MH197154	Kaczmarek et al. (2018a)
Mesobiotus radiatus	MH197153	MH197152	MH195147	MH197267	Stec et al. (2018e)
Mesobiotus romani	MH197158	MH197151	MH195149	MH197150	Roszkowska et al. (2018)
Minibiotus ioculator	MT023999	MT024041	MT023412	MT024000	Stec et al. (2020a)
Minibiotus pentannulatus	MT023998	MT024042	MT023413	MT024001	Stec et al. (2020a)
Paramacrobiotus areolatus	MH664931	MH664948	MH675998	MH666080	Stec et al. (2020d)
Paramacrobiotus fairbanksi	MH664942	MH664959	MH676012	MH666091	Stec et al. (2020d)
Paramacrobiotus lachowskae	MF568532	MF568533	MF568534	MF568535	Stec et al. (2018f)
Paramacrobiotus tonollii	MH664946	MH664963	MH676018	MH666096	Stec et al. (2020d)
Richtersius coronifer	MH681760	MH681757	MH676053	MH681763	Stec et al. (2020e)
Sisubiotus spectabilis FI	MN888371	MN888357	MN888322	MN888331	Stec et al. (2021)
			MN888323		
Sisubiotus spectabilis NO	MN888372	MN888364	MN888324	MN888344	Stec et al. (2021)
Tenuibiotus danilovi	MN888377	MN888362	MN888329	MN888349	Stec et al. (2021)
Tenuibiotus tenuiformis	MN888378	MN888363	MN888330	MN888350	Stec et al. (2021)
Tenuibiotus zandrae	MN443040	MN443035	MN444827	MN443038	Stec et al. (2020b)

Class: Eutardigrada Richters, 1926

Order: Parachela Schuster et al., 1980 (restored by Morek et al. 2020)

Superfamily: Macrobiotoidea Thulin, 1928 (in Marley et al. 2011)

Family: Macrobiotidae Thulin, 1928

Genus: *Macrobiotus* Schultze C.A.S., 1834

Macrobiotus annewintersae Vecchi & Stec, sp. nov.

http://zoobank.org/05EFF40C-9238-49B8-9D79-7986979F674D

Tables 3, 4, Figures 1–8, Suppl. material 1

Etymology. We dedicate this species to MV friend and colleague Dr. Anne Winters, evolutionary ecologist, who collected the sample in which the new species was found.

Material examined. 146 animals and 56 eggs. Specimens mounted on microscope slides in Hoyer's medium (93 animals + 38 eggs), fixed on SEM stubs (51+18), and processed for DNA sequencing (2+0).

Type locality. 32°21'05"N, 89°56'30"W; 106 m asl: suburban area of Jackson, Mississippi, USA; mixed leaf litter on ground; coll. December 2019 by Anne Winters.

Type depositories. Holotype ♀ (slide US.084.01 with 10 paratypes) and 63 paratypes (slides: US.084.*, where the asterisk can be substituted by any of the following numbers: 02–05) and 20 eggs (slides US.084.*: 06–08) are deposited at the Institute of Zoology and Biomedical Research, Jagiellonian University (Gronostajowa 9, 30-387, Kraków, Poland). Additional paratypes (71 animals + 29 eggs) (slides: S207_SL*: 1–15; SEM stubs: S207_Stub*:1–4) are deposited at the Department of Biological and Environmental Sciences, University of Jyväskylä (Survontie 9C, 40500, Jyväskylä, Finland).

Description of the new species. ***Animals*** (measurements and statistics in Table 3):

In live animals, body translucent in smaller specimens and opaque whitish in larger animals; transparent after fixation in Hoyer's medium (Figure 1). Eyes present in live animals and after fixation in Hoyer's medium. Small roundish cuticular pores on the dorsal and lateral cuticle, as well as on the external cuticle of all legs (0.2–0.6 µm in diameter), visible under both PCM and SEM (Figures 1B, C, 2D). On the dorsal surface, pores are absent between cuticle folds and arranged in loose belts (Figure 1C). Pores sparse on the ventral surface and visible only under SEM (Figure 8C). Patches of fine granulation, on the external surface of legs I–III as well as on the dorsal and dorso-lateral sides of legs IV, visible in PCM (Fig-

Table 3. Measurements [in µm] of selected morphological structures of individuals of *Macrobiotus annewintersae* **sp. nov.** mounted in Hoyer's medium (N–number of specimens/structures measured, RANGE refers to the smallest and the largest structure among all measured specimens; SD–standard deviation).

Character	N	Range						Mean		Sd		Holotype	
		µm			***pt***			µm	***pt***	µm	***pt***	µm	***Pt***
Body length	29	287	–	441	*934*	–	*1226*	371	*1074*	46	*84*	434	*1226*
Buccal tube													
Buccal tube length	28	27.1	–	40.4		–		34.3	–	3.1	–	35.4	–
Stylet support insertion point	28	21.2	–	32.0	*76.8*	–	*81.6*	27.2	*79.4*	2.4	*1.3*	27.5	*77.7*
Buccal tube external width	29	3.4	–	6.1	*12.5*	–	*17.0*	4.7	*13.8*	0.6	*1.0*	5.4	*15.3*
Buccal tube internal width	29	1.9	–	4.5	*6.8*	–	*11.5*	3.2	*9.4*	0.6	*1.1*	3.3	*9.3*
Ventral lamina length	22	16.0	–	26.1	*49.4*	–	*64.5*	20.1	*58.8*	2.2	*3.0*	21.9	*61.9*
Placoid lengths													
Macroplacoid 1	28	6.3	–	10.3	*20.9*	–	*28.9*	8.3	*24.4*	1.0	*1.8*	9.4	*26.6*
Macroplacoid 2	30	3.6	–	6.8	*12.6*	–	*18.5*	5.3	*15.2*	0.8	*1.6*	5.6	*15.8*
Microplacoid	30	1.6	–	4.1	*4.7*	–	*11.5*	2.6	*7.7*	0.6	*1.6*	2.9	*8.2*
Macroplacoid row	26	10.9	–	17.6	*38.8*	–	*49.4*	14.8	*43.6*	1.8	*2.8*	16.6	*46.9*
Placoid row	26	13.7	–	22.3	*48.8*	–	*62.6*	18.5	*54.5*	2.2	*3.6*	20.7	*58.5*
Claw 1 heights													
External primary branch	24	7.4	–	11.0	*22.7*	–	*30.4*	9.5	*27.6*	0.8	*2.0*	10.4	*29.4*
External secondary branch	22	5.7	–	8.7	*18.6*	–	*24.2*	7.6	*21.6*	0.7	*2.0*	8.5	*24.0*
Internal primary branch	25	7.3	–	10.5	*21.8*	–	*28.4*	8.7	*25.5*	0.7	*1.9*	9.6	*27.1*
Internal secondary branch	23	5.4	–	8.6	*16.7*	–	*22.5*	7.0	*20.1*	0.7	*1.4*	7.5	*21.2*
Claw 2 heights													
External primary branch	26	7.2	–	11.6	*25.6*	–	*32.5*	10.0	*29.1*	1.0	*1.9*	11.0	*31.1*
External secondary branch	25	6.3	–	9.6	*18.9*	–	*26.3*	8.0	*23.0*	0.8	*2.0*	9.3	*26.3*
Internal primary branch	28	7.0	–	11.6	*23.8*	–	*30.8*	9.4	*27.1*	0.9	*1.9*	9.8	*27.7*
Internal secondary branch	26	5.4	–	9.0	*15.6*	–	*24.3*	7.1	*20.5*	0.9	*2.1*	8.6	*24.3*
Claw 3 heights													
External primary branch	25	8.3	–	11.4	*25.8*	–	*31.0*	9.9	*28.8*	0.9	*1.7*	10.9	*30.8*
External secondary branch	24	5.9	–	9.3	*19.1*	–	*27.2*	7.8	*22.6*	1.0	*2.2*	9.3	*26.3*
Internal primary branch	26	7.0	–	10.7	*20.3*	–	*28.8*	9.0	*26.3*	0.9	*1.8*	9.4	*26.6*
Internal secondary branch	24	5.2	–	8.4	*16.5*	–	*23.1*	7.1	*20.7*	0.9	*1.8*	7.7	*21.8*
Claw 4 heights													
Anterior primary branch	26	8.2	–	12.5	*25.0*	–	*35.3*	10.4	*30.6*	1.1	*2.5*	12.5	*35.3*
Anterior secondary branch	25	5.2	–	9.4	*14.3*	–	*26.3*	7.7	*22.7*	0.8	*2.5*	9.3	*26.3*
Posterior primary branch	25	9.2	–	14.5	*29.5*	–	*37.6*	11.5	*33.5*	1.1	*2.4*	12.7	*35.9*
Posterior secondary branch	23	6.9	–	10.4	*19.9*	–	*31.6*	8.4	*24.7*	0.9	*2.8*	?	*?*

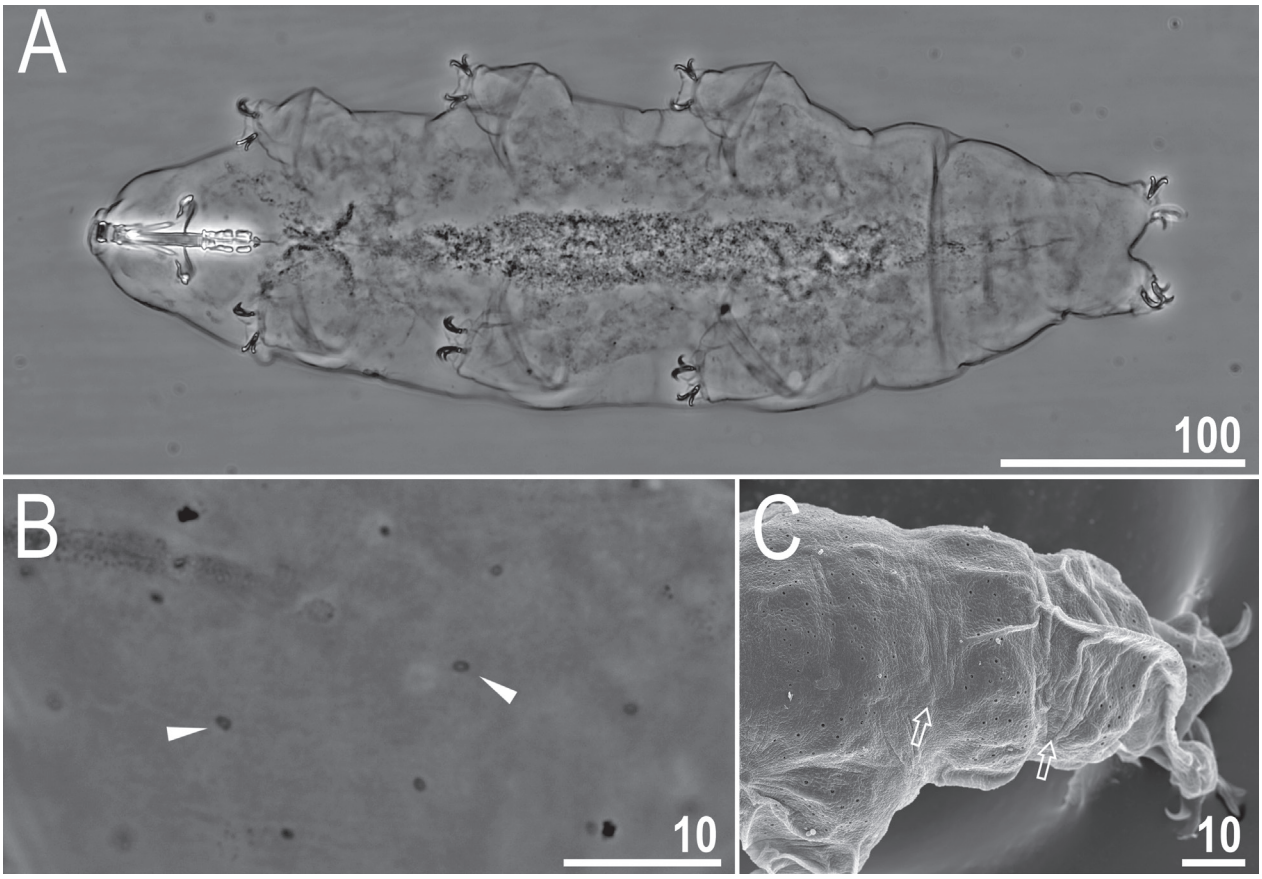

Figure 1. *Macrobiotus annewintersae* sp. nov. – habitus and cuticular pores: **A.** Dorso-ventral view of the body (Holotype ♀;, PCM); **B, C.** Cuticular pores on the dorsal part of the body under PCM and under SEM, respectively. Arrowheads indicate pores and empty arrows indicate places on dorsal cuticle without pores. Scale bars in μm.

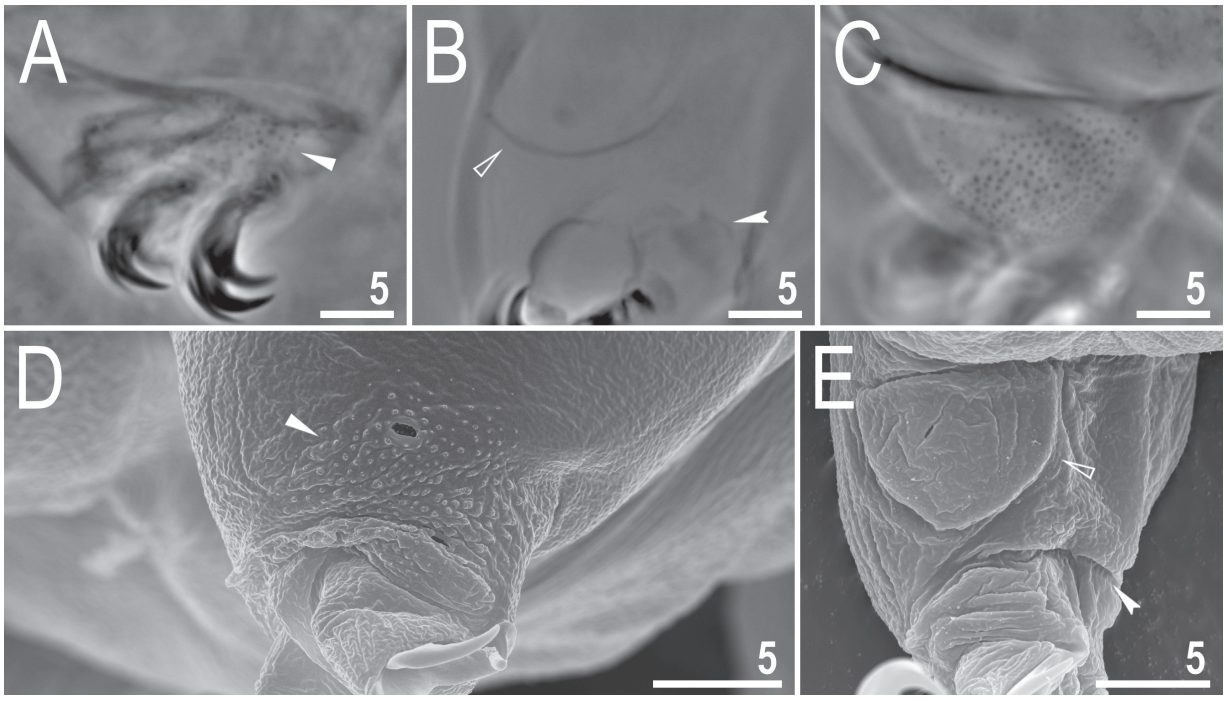

Figure 2. *Macrobiotus annewintersae* sp. nov. – cuticular structures on legs: **A.** External granulation on leg III under PCM; **B.** A cuticular bulge (pulvinus) on the internal surface of leg III under PCM; **C.** Granulation on leg IV under PCM; **D.** External granulation on leg III under SEM; **E.** A cuticular bulge (pulvinus) on the internal surface of leg III under SEM. Filled flat arrowheads indicate the granulation patch, empty flat arrowheads indicate pulvinus and filled indented arrowheads indicate muscle attachments. C assembled from several photos. Scale bars in μm.

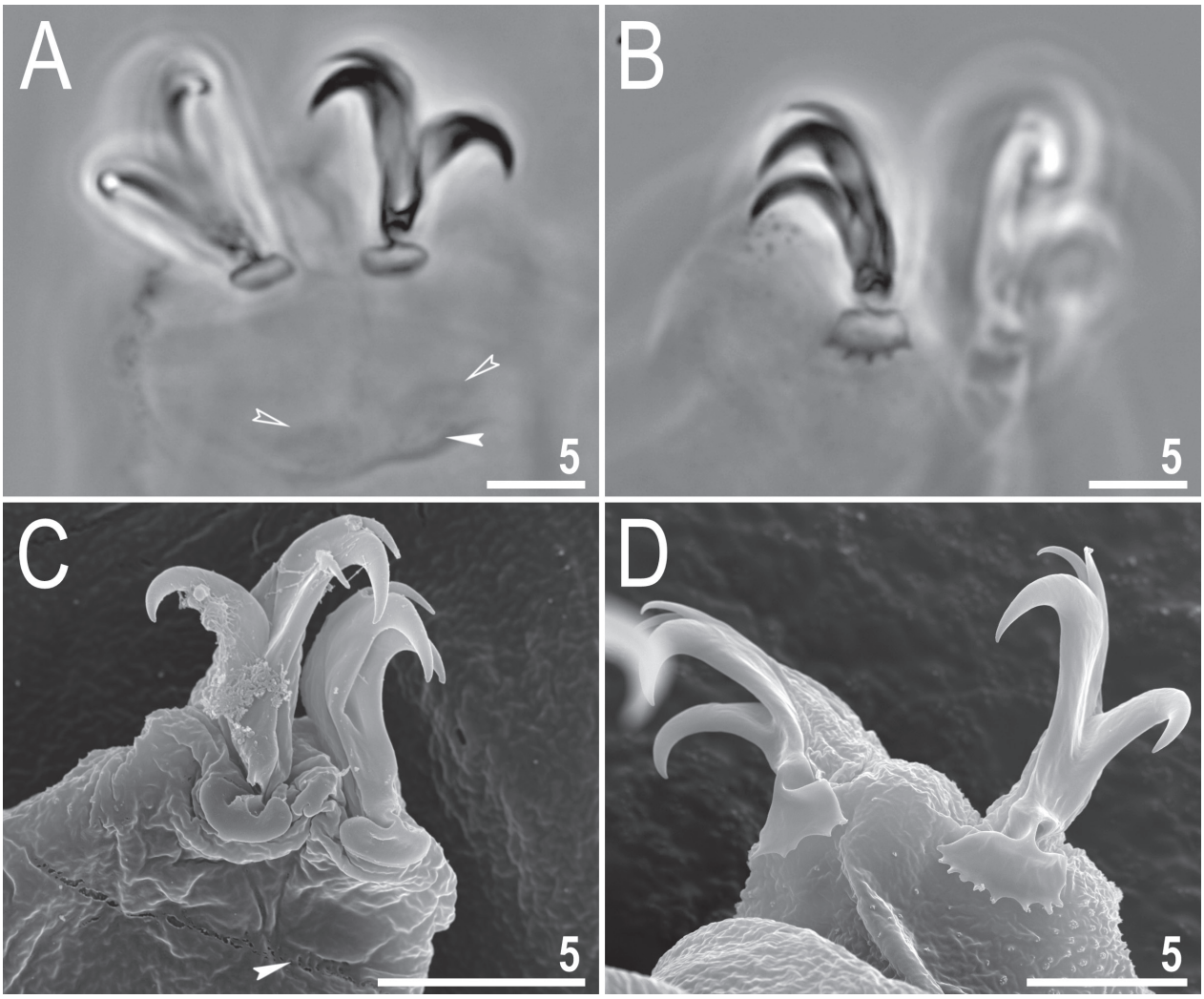

Figure 3. *Macrobiotus annewintersae* sp. nov. – claws: **A, B.** Claws III and IV, respectively, under PCM; **C, D.** Claws III and IV, respectively, under SEM. Filled indented arrowheads indicate double muscle attachments under the claws, empty indented arrowheads indicate a faintly visible divided cuticular bar. A and B assembled from several photos. Scale bars in μm.

ure 2A, C) and SEM (Figure 2D). A pulvinus is present on the internal surface of legs I–III (Figure 2B, E).

Claws Y-shaped, of the *hufelandi* type. Primary branches with distinct accessory points, a common tract, and an evident stalk connecting the claw to the lunula (Figure 3). The lunulae I–III are smooth (Figure 3A, C), whereas lunulae IV are dentate (Figure 3B, D). A divided cuticular bar with double muscle attachments are poorly visible under PCM (Figure 3A).

Mouth antero-ventral. Bucco-pharyngeal apparatus of the *Macrobiotus* type (Figure 4) with ventral lamina and ten peribuccal lamellae. The stylet furcae typically-shaped, the basal portion is enlarged and has two caudal branches with thickened, swollen, rounded apices. Under PCM, the oral cavity armature is of the *patagonicus* type, *i.e.*, with only the second and third bands of teeth visible (Figure 4B, C). However, under SEM the first band of teeth is visible and composed of one row of very small cones situated anteriorly in the oral cavity, just behind the bases of the peribuccal lamellae (Figure 5). The second band of teeth is situated between the ring fold and the third band of teeth and composed of 3–4 rows of teeth visible in PCM as granules (Figure 4B, C). The third band of teeth is divided into a dorsal (Figure 4B) and a ventral portion (Figure 4C). Under PCM, the dorsal teeth are seen as three distinct transverse ridges whereas the ventral teeth appear as two separate lateral transverse ridges between which one big tooth (sometimes circular in PCM) is visible (Figure 4B, C).

Pharyngeal bulb spherical, with triangular apophyses, two rod-shaped macroplacoids and a drop-shaped microplacoid (Figure 4A, D, E). The macroplacoid length sequence is 2<1. The first and the second macroplacoid have a central and a subterminal constriction, respectively (Figure 4D, E).

Eggs (measurements and statistics in Table 4):

The surface between processes is of the *persimilis* type, *i.e.*, with a continuous smooth chorion, never with pores or reticulum (Figures 6, 7). Under PCM the surface between the processes is covered with wrinkles that appear as dark thickenings/striae, whereas under SEM the surface appears clearly wrinkled (Figures 6, 7). Processes

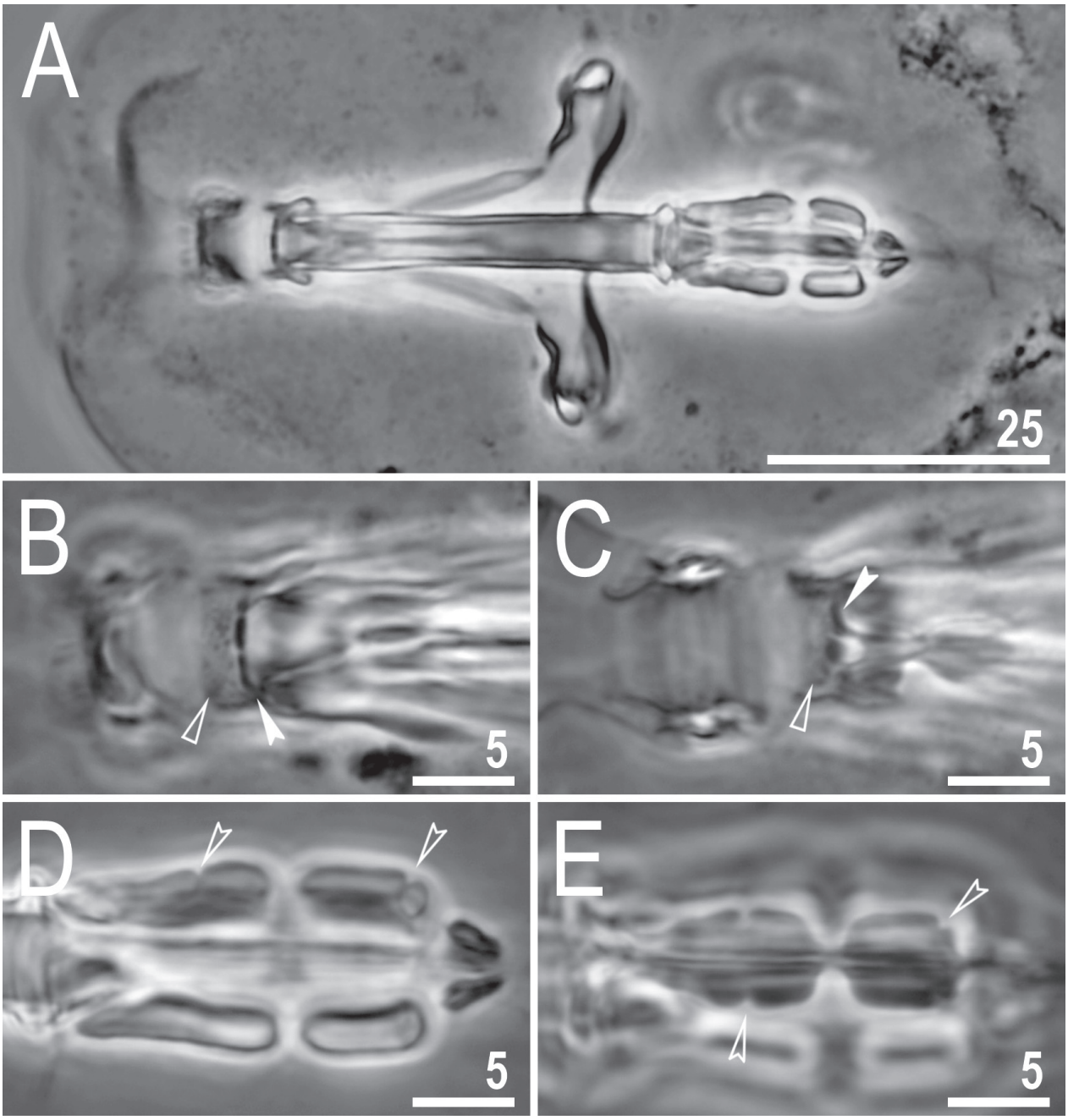

Figure 4. *Macrobiotus annewintersae* sp. nov. – buccal apparatus and the oral cavity armature under PCM: **A.** Dorso-ventral view of the entire buccal apparatus; **B, C.** Oral cavity armature in dorsal and ventral view, respectively; **D, E.** Placoid morphology in dorsal and ventral view, respectively. Empty flat arrowheads indicate the second band of teeth, filled indented arrowheads indicate the third band of teeth in the oral cavity, and empty indented arrowheads indicate central constriction in the first macroplacoid and subterminal constriction in the second macroplacoid. **A, D** and **E** assembled from several photos. Scale bars in µm.

are of a modified *hufelandi* type (Figures 6, 7). The proper terminal disc is absent and instead 2–8 thick tentacular arms (typically 5–6) are present in the distal part of the process (Figures 6, 7). The tentacular arms present bubble-like structures (visible in PCM). Under SEM, each tentacular arm is distally divided into many irregular digitations that are sometime covered with micro-granulation (Figure 7C–F). Also, under SEM micro-pores can be seen on the egg surface between the processes and around the process bases (Figure 7C, E).

Reproduction / Sexual dimorphism. The species is dioecious. Spermathecae in females as well as testis in males, clearly visible under PCM up to 24 hours after mounting in Hoyer's medium, have been found to be filled with spermatozoa (Figure 8A, B). The species exhibits secondary sexual dimorphism in the form of clearly visible lateral gibbosities on the hind legs in males (Figure 8B, C).

DNA sequences. 18S rRNA: GenBank: MW588024–MW588025; 659 and 664 bp long.

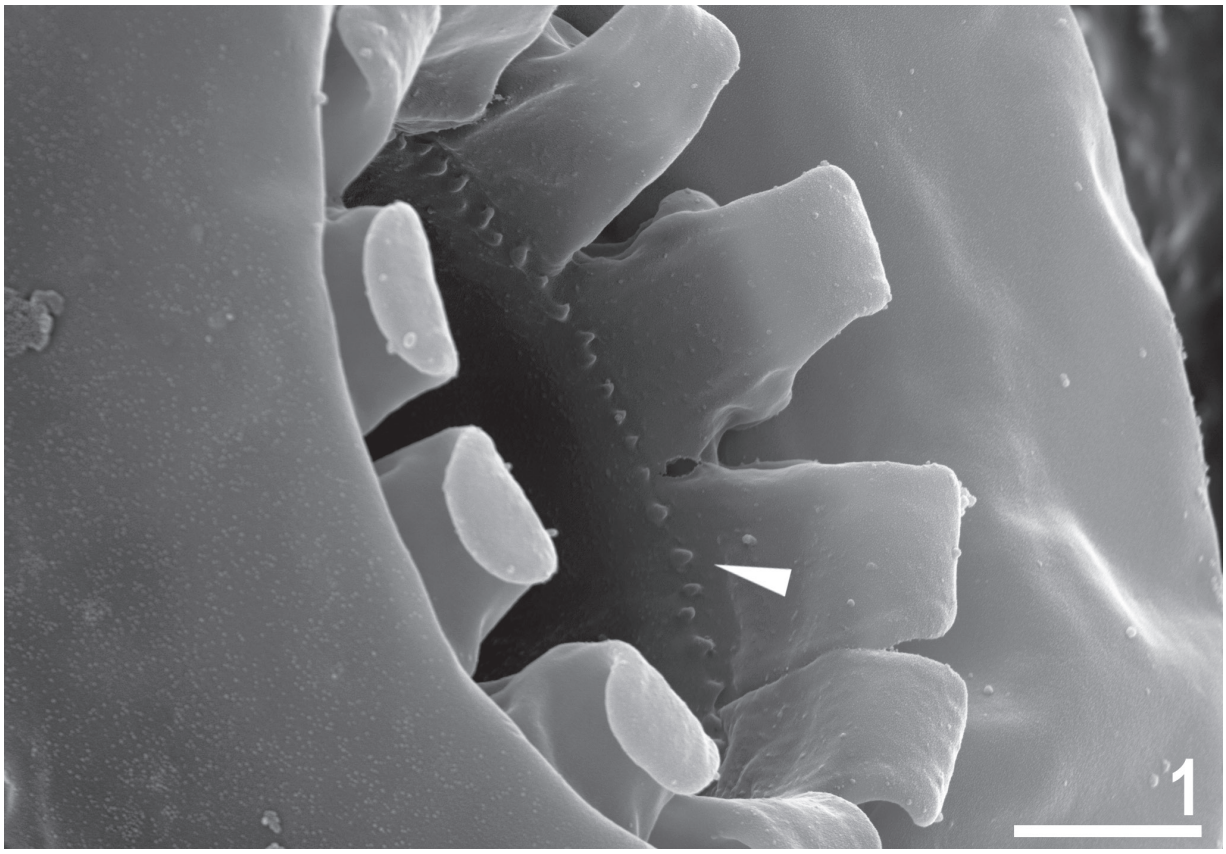

Figure 5. *Macrobiotus annewintersae* sp. nov. – anterior view of the mouth opening under SEM. Filled flat arrowhead indicates the first band of teeth. Scale bar in µm.

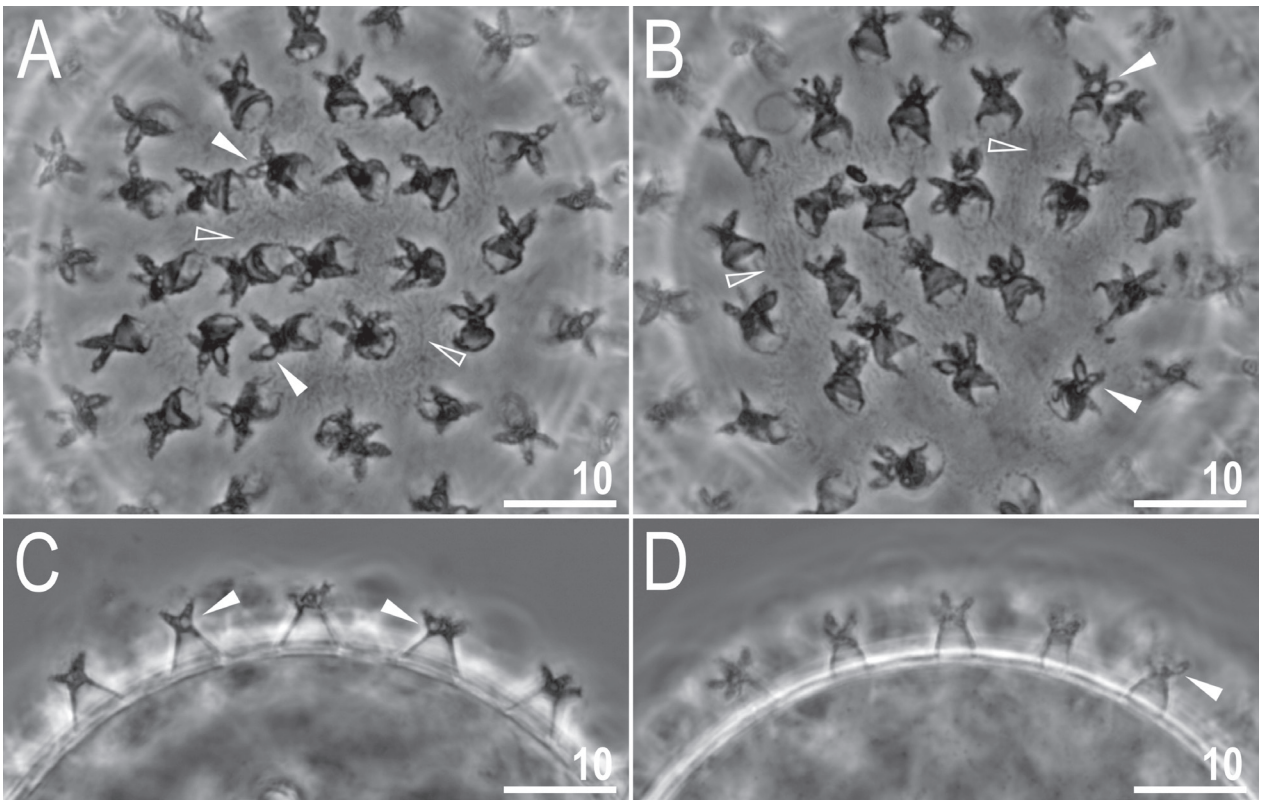

Figure 6. *Macrobiotus annewintersae* sp. nov. – egg chorion morphology under PCM: **A, B.** Egg surface; **C, D.** Midsection of the processes. Filled flat arrowheads indicate bubble-like structures within tentacular arms in the distal portion of the egg processes and empty flat arrowheads indicate dark thickenings/striae on the egg surface between processes. Scale bars in µm.

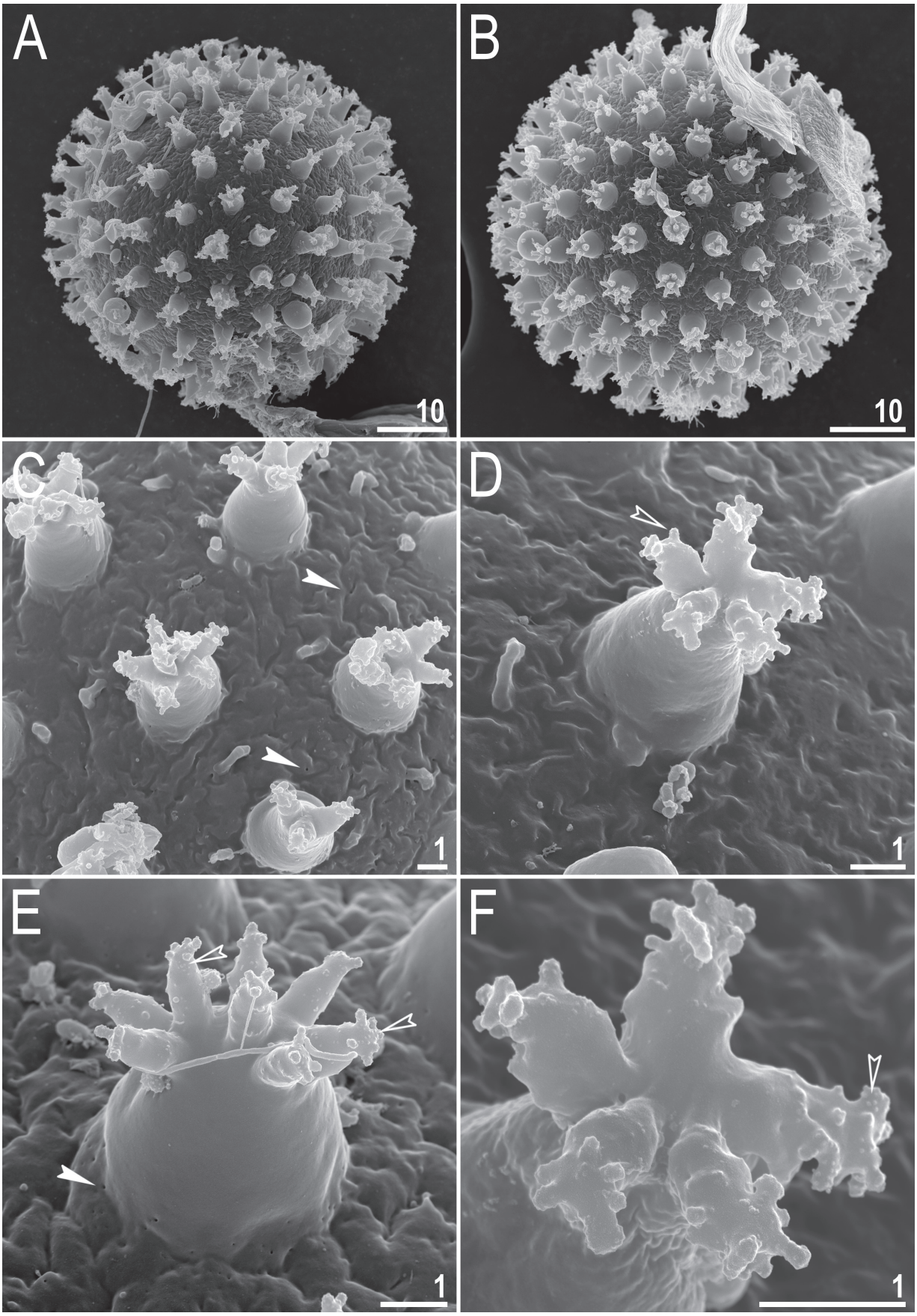

Figure 7. *Macrobiotus annewintersae* sp. nov. – egg chorion morphology under SEM: **A, B.** Entire egg; **C–E.** Details of the egg processes and egg surface between them; **F.** Details of the tentacular arms in the distal portion of each egg process. Filled indented arrowheads indicate micropores and empty indented arrowheads indicate lobes in tentacular arms covered by micro-granulation. Scale bars in μm.

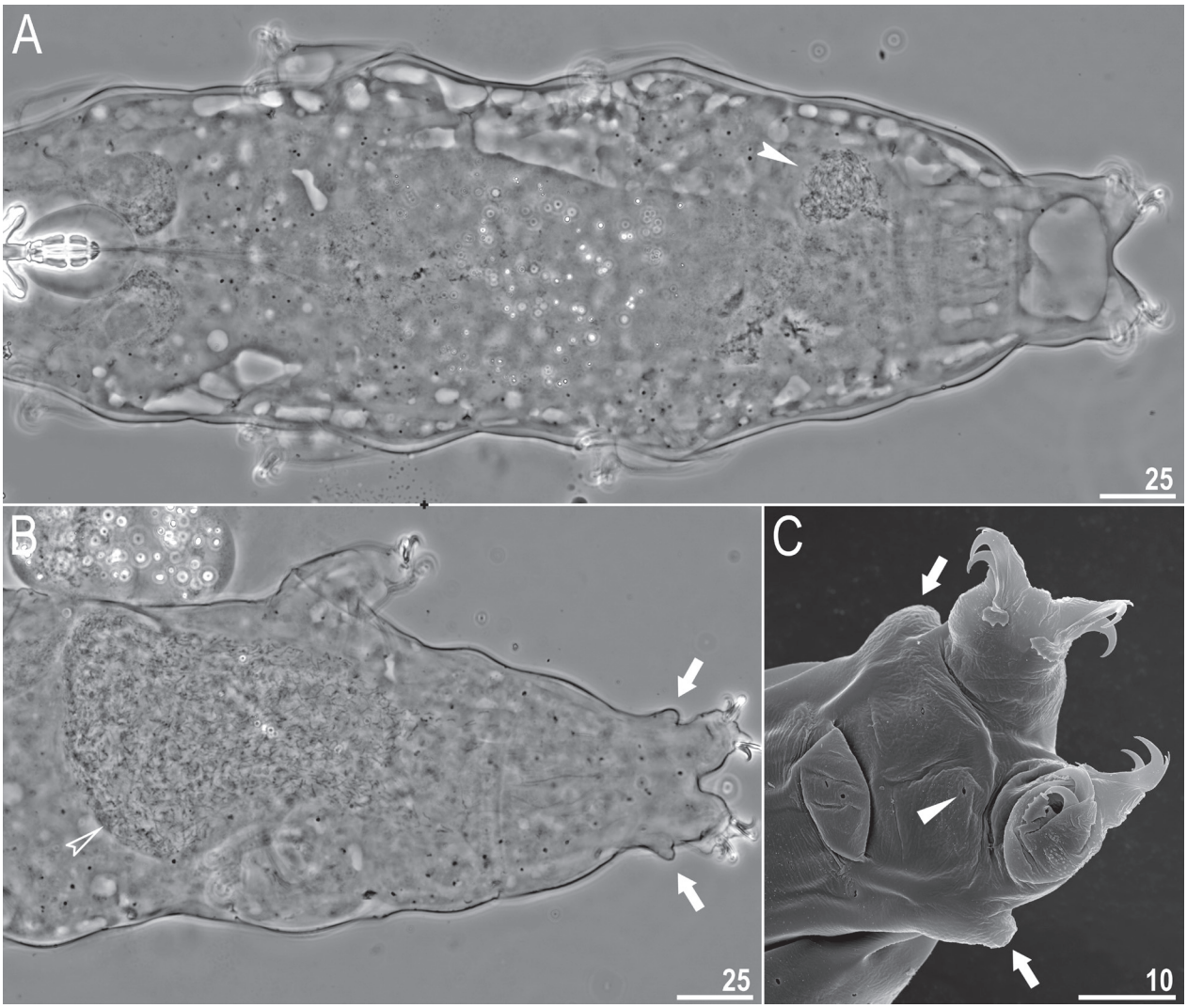

Figure 8. *Macrobiotus annewintersae* sp. nov. – reproduction: **A.** Female under PCM; **B.** Male under PCM; **C.** Male under SEM. Filled indented arrowhead indicates spermathecae filled with spermatozoa, empty indented arrowhead indicates male's testis, arrows indicate lateral gibbosities on legs IV and filled flat arrowhead indicates cuticular pore on the ventral side of the body. Scale bars in µm.

Table 4. Measurements [in µm] of selected morphological structures of the eggs of *Macrobiotus annewintersae* sp. nov. mounted in Hoyer's medium (N–number of eggs/structures measured, RANGE refers to the smallest and the largest structure among all measured specimens; SD–standard deviation).

Character	N	Range			Mean	Sd
egg bare diameter	20	59.8	–	76.7	66.1	3.7
Egg full diameter	20	69.8	–	87.1	75.7	4.6
Process height	63	4.2	–	7.3	5.8	0.7
Process base width	63	2.4	–	5.9	4.1	0.7
Process base/height ratio	63	52%	–	100%	71%	10%
Terminal disc width	63	2.8	–	6.7	4.4	0.9
Inter-process distance	63	2.3	–	6.9	4.2	0.9
Number of processes on the egg circumference	20	21	–	28	24.4	1.7

28S rRNA: GenBank: MW588030–MW588031; 679 and 703 bp long.

ITS-2: GenBank: MW588018–MW588019; 298 bp long.

COI: GenBank: MW593927–MW593928; 532 and 535 bp long.

***Phenotypic differential diagnosis*.** By having an egg chorion of the *persimilis type* (smooth or wrinkled chorion) and by having thick tentacular arms instead of a proper terminal disc on the distal part of egg processes, *M. annewintersae* sp. nov. resembles only one species: *Macrobiotus anemone* Meyer, Domingue & Hinton, 2014 from USA. However, the new species differs specifically from:

- ***M. anemone*** by having eyes (absent in *M. anemone*), by the presence of granulation on all legs (absent in *M. anemone*), by having the oral cavity armature (OCA) of the *patagonicus* type (*maculatus* type – only the third band of teeth visible under light microscope – in *M. anemone*), by the presence of dentate lunulae in legs IV (smooth lunulae in legs IV in *M. anemone*), by having the thick tentacular arms in the distal part of the processes filled with bubble-like structures (tentacular arms solid in *M. anemone*, Figure 17) and by lacking a cavity between the process trunk and tentacular arms that

appears in PCM as a clearly refracting dot (the cavity present in *M. anemone*, Figure 17).

Macrobiotus rybaki Stec & Vecchi, sp. nov.

http://zoobank.org/FC73B03E-E5BF-4597-822F-BBAC95F1FFEB

Tables 5, 6, Figures 9–16, SM.02

Etymology. We dedicate this species to the singer, composer, musician, actor and the 2009 Eurovision Song Contest winner, Alexander Rybak.

Material examined. 173 animals and 37 eggs. Specimens mounted on microscope slides in Hoyer's medium (156 animals + 32 eggs), fixed on SEM stubs (15+5), and processed for DNA sequencing (2+0).

Type locality. 35°15'00"N, 23°49'28"E; 30 m asl: Omalos, Crete, Greece; moss on rock in a xeric shrubland; coll. June 2015 by Małgorzata Mitan and Małgorzata Osielczak.

Type depositories. Holotype ♂ (slide GR.011.11 with 11 paratypes) and 160 paratypes (slides: GR.011.*, where the asterisk can be substituted by any of the following numbers: 02–08, 10–13, 15–16; SEM stub: 18.10) and 37 eggs (slides GR.011.*: 01, 09, 14; SEM stub: 18.10) are deposited at the Institute of Zoology and Biomedical Research, Jagiellonian University (Gronostajowa 9, 30-387, Kraków, Poland).

Description of the new species. ***Animals*** (measurements and statistics in Table 5):

In live animals, body translucent in smaller specimens and opaque whitish in larger animals; transparent after fixation in Hoyer's medium (Figure 9A). Eyes present in live animals and after fixation in Hoyer's medium. Elliptical cuticular pores (0.6–1.5 µm in length) present all over the body and clearly visible under both PCM and SEM (Figures 9B–D, 10). Patches of fine granulation on the external surface of legs I–III as well as on the dorsal and dorso-lateral sides of legs IV clearly visible under both PCM and SEM (Figure 10A, B, E, F). A pulvinus is present on the internal surface of legs I–III (Figure 10C, D).

Claws Y-shaped, of the *hufelandi* type. Primary branches with distinct accessory points, a common tract, and an evident stalk connecting the claw to the lunula (Figure 11). The lunulae I–III are smooth (Figure 11A, D, E), whereas lunulae IV are dentate (Figure 11B, C, F). A divided cuticular bar and doubled muscle attachments are visible under PCM (Figures 10C, D, 11A, D, E).

Mouth antero-ventral. Bucco-pharyngeal apparatus of the *Macrobiotus* type (Figure 12), with ventral lamina and ten peribuccal lamellae (Figure 13A). The stylet furcae

Table 5. Measurements [in µm] of selected morphological structures of individuals of *Macrobiotus rybaki* sp. nov. mounted in Hoyer's medium (N–number of specimens/structures measured, RANGE refers to the smallest and the largest structure among all measured specimens; SD–standard deviation).

Character	N	Range						Mean		Sd		Holotype	
		µm			pt			µm	pt	µm	pt	µm	pt
Body length	30	320	–	520	*915*	–	*1190*	424	*1054*	39	*67*	436	*1093*
Buccal tube													
Buccal tube length	30	34.9	–	44.4		–		40.2	–	2.3	–	39.9	–
Stylet support insertion point	30	25.8	–	33.1	*73.0*	–	*75.4*	29.7	*73.9*	1.7	*0.6*	30.1	*75.4*
Buccal tube external width	30	4.4	–	6.6	*12.3*	–	*15.6*	5.5	*13.7*	0.5	*0.8*	5.1	*12.8*
Buccal tube internal width	30	2.8	–	5.5	*7.0*	–	*13.3*	4.6	*11.4*	0.5	*1.0*	2.8	*7.0*
Ventral lamina length	27	21.5	–	28.9	*59.4*	–	*65.9*	25.6	*63.7*	1.8	*1.7*	24.5	*61.4*
Placoid lengths													
Macroplacoid 1	30	8.2	–	13.1	*23.5*	–	*30.1*	10.8	*26.8*	1.1	*1.8*	9.5	*23.8*
Macroplacoid 2	30	5.8	–	8.0	*15.3*	–	*19.5*	6.9	*17.1*	0.6	*1.1*	6.2	*15.5*
Microplacoid	30	1.9	–	3.8	*4.3*	–	*9.2*	2.7	*6.8*	0.4	*1.0*	2.5	*6.3*
Macroplacoid row	30	15.4	–	22.1	*42.6*	–	*51.2*	18.7	*46.5*	1.7	*2.5*	17.0	*42.6*
Placoid row	30	18.2	–	25.2	*51.1*	–	*61.0*	22.1	*55.0*	1.8	*2.7*	20.4	*51.1*
Claw 1 heights													
External primary branch	27	10.1	–	15.7	*26.8*	–	*36.2*	12.5	*31.0*	1.2	*2.1*	12.2	*30.6*
External secondary branch	26	8.0	–	12.1	*21.9*	–	*28.9*	9.9	*24.5*	1.0	*1.9*	9.4	*23.6*
Internal primary branch	27	9.4	–	14.8	*26.1*	–	*33.9*	11.9	*29.5*	1.2	*1.8*	11.8	*29.6*
Internal secondary branch	27	7.2	–	10.8	*18.6*	–	*26.9*	9.2	*22.8*	1.1	*2.1*	9.0	*22.6*
Claw 2 heights													
External primary branch	30	10.5	–	15.0	*30.1*	–	*37.4*	13.1	*32.7*	1.0	*1.7*	12.4	*31.1*
External secondary branch	28	8.2	–	12.8	*22.9*	–	*31.4*	10.5	*26.0*	1.1	*2.1*	9.9	*24.8*
Internal primary branch	30	10.1	–	14.6	*26.6*	–	*35.4*	12.6	*31.3*	1.0	*1.9*	11.8	*29.6*
Internal secondary branch	30	7.5	–	11.8	*19.4*	–	*29.6*	9.9	*24.6*	1.1	*2.5*	8.5	*21.3*
Claw 3 heights													
External primary branch	28	11.5	–	15.8	*29.6*	–	*38.2*	13.4	*33.5*	1.2	*2.2*	12.3	*30.8*
External secondary branch	25	8.5	–	13.3	*23.2*	–	*32.1*	10.6	*26.7*	1.2	*2.5*	9.8	*24.6*
Internal primary branch	29	10.6	–	15.2	*28.9*	–	*36.2*	12.9	*32.2*	1.1	*1.9*	11.7	*29.3*
Internal secondary branch	29	7.2	–	11.8	*20.6*	–	*29.8*	10.0	*24.9*	1.1	*2.3*	9.4	*23.6*
Claw 4 heights													
Anterior primary branch	28	12.5	–	17.4	*34.2*	–	*44.9*	15.7	*39.2*	1.4	*3.2*	15.4	*38.6*
Anterior secondary branch	23	7.7	–	12.9	*20.6*	–	*31.4*	10.7	*26.6*	1.4	*3.2*	11.2	*28.1*
Posterior primary branch	26	13.2	–	18.8	*35.4*	–	*46.3*	16.8	*41.8*	1.4	*3.1*	17.3	*43.4*
Posterior secondary branch	25	9.0	–	13.1	*24.1*	–	*33.8*	11.7	*29.2*	1.1	*2.6*	11.9	*29.8*

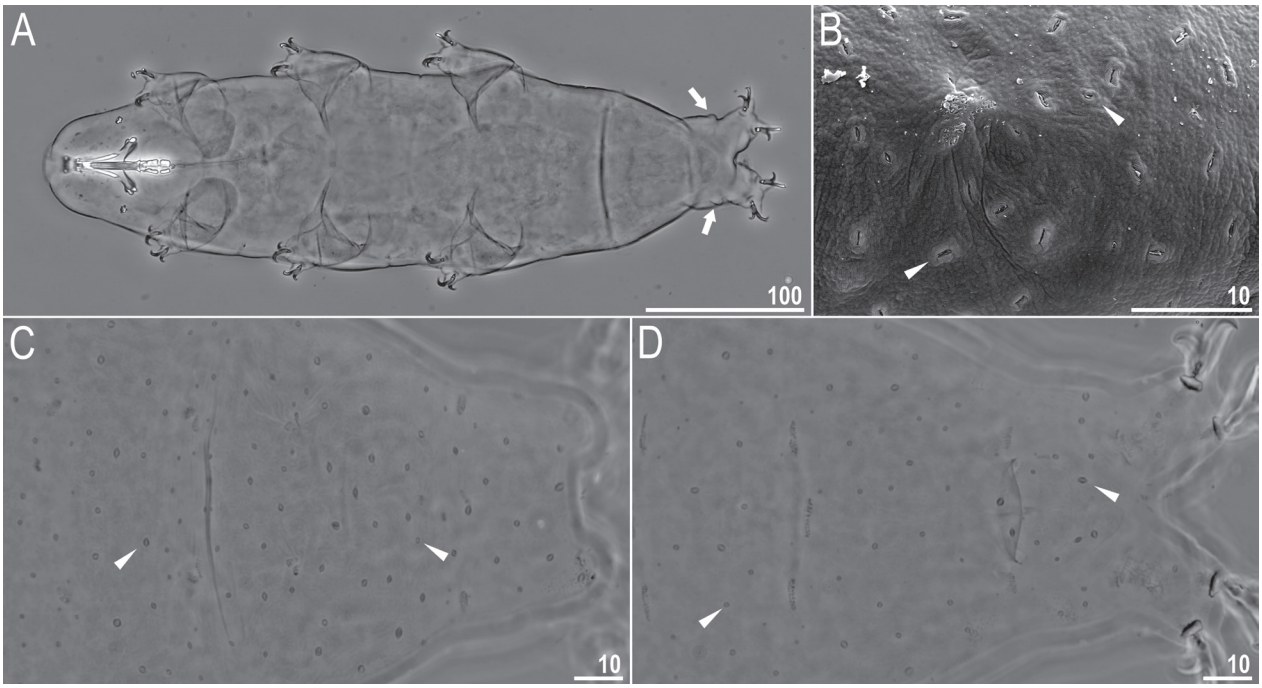

Figure 9. *Macrobiotus rybaki* sp. nov. – habitus and cuticular pores: **A.** Dorso-ventral view of the body (Holotype ♂; Hoyer's medium, PCM); **B.** Cuticular pores on the dorsal part of the body under SEM; **C, D.** Cuticular pores on the dorsal and ventral part of the body under PCM, respectively. Filled arrows indicate lateral gibbosities. Arrowheads indicate elliptical pores. Scale bars in µm.

typically-shaped, the basal portion is enlarged and has two caudal branches with thickened, swollen, rounded apices. Under PCM, the oral cavity armature is of the *patagonicus* type, *i.e.*, with only the second and third bands of teeth visible (Figure 12B, C). However, under SEM the first band of teeth is visible as a row of irregularly distributed small teeth situated anteriorly in the oral cavity, just behind the bases of the peribuccal lamellae (Figure 13A, B). The second band of teeth is situated between the ring fold and the third band of teeth and comprised of 3–4 rows of teeth faintly visible in PCM (Figure 12B, C) and visible as cones in SEM (Figure 13A). Teeth of the second band are larger than those in the first band. The teeth of the third band are located within the posterior portion of the oral cavity, between the second band of teeth and the buccal tube opening (Figures 12B, C, 13A, B). The third band of teeth is divided into a dorsal and the ventral portion. Under both PCM and SEM, the dorsal teeth are seen as three distinct transverse ridges (Figures 12B, 13A). The ventral teeth appear as two separate lateral transverse ridges between which one conical medial tooth (roundish in PCM) is visible (Figures 12C, 13B). Lateral cribrose area present in the buccal tube behind the third band of teeth (Figure 13B). Pharyngeal bulb spherical, with triangular apophyses, three anterior cuticular spikes (typically only two are visible in any given plane), two rod-shaped macroplacoids and a drop-shaped microplacoid (Figures 12A, D, E). The macroplacoid length sequence is 2<1. The first macroplacoid has a weak central constriction, whereas the second is weakly constricted only subterminally (Figures 12D, E).

Eggs (measurements and statistics in Table 6):

Table 6. Measurements [in µm] of selected morphological structures of the eggs of *Macrobiotus rybaki* sp. nov. mounted in Hoyer's medium (N–number of eggs/structures measured, RANGE refers to the smallest and the largest structure among all measured specimens; SD–standard deviation).

Character	N	Range			Mean	Sd
Egg bare diameter	14	68.7	–	93.4	76.2	7.6
Egg full diameter	14	83.6	–	107.9	94.1	7.9
Process height	42	6.7	–	13.4	9.2	1.5
Process base width	42	4.4	–	9.6	6.9	1.0
Process base/height ratio	42	52%	–	99%	76%	12%
Terminal disc width	42	1.3	–	4.2	2.3	0.7
Inter-process distance	42	1.4	–	4.5	2.7	0.8
Number of processes on the egg circumference	14	25	–	34	28.1	3.0

The surface between processes is of the *hufelandi* type, *i.e.*, covered with a reticulum (Figures 14A, B, 15A–E). Peribasal meshes of slightly larger diameter compared to interbasal meshes (Figures 14A, B, 15A–D). Typically, the reticulation between neighbouring processes is composed of two rows of peribasal meshes and with a third row of smaller mashes interposed (the third row sometimes missing) (Figures 14A, B, 15A–D). Mesh diameter is usually larger than the mesh walls and nodes (Figures 14A, B, 15A–D). The meshes are 0.4–1.4 µm in diameter, with roundish irregular shape. The pillars connecting the reticulum with the chorion surface are visible only under SEM (Figure 15C). The bases of the processes are surrounded by cuticular thickenings that merge into the bars and nodes of the reticulum (Figure 15C, D). These basal thickenings appear under PCM as short dark projections around the process bases (Figure 14A, B).

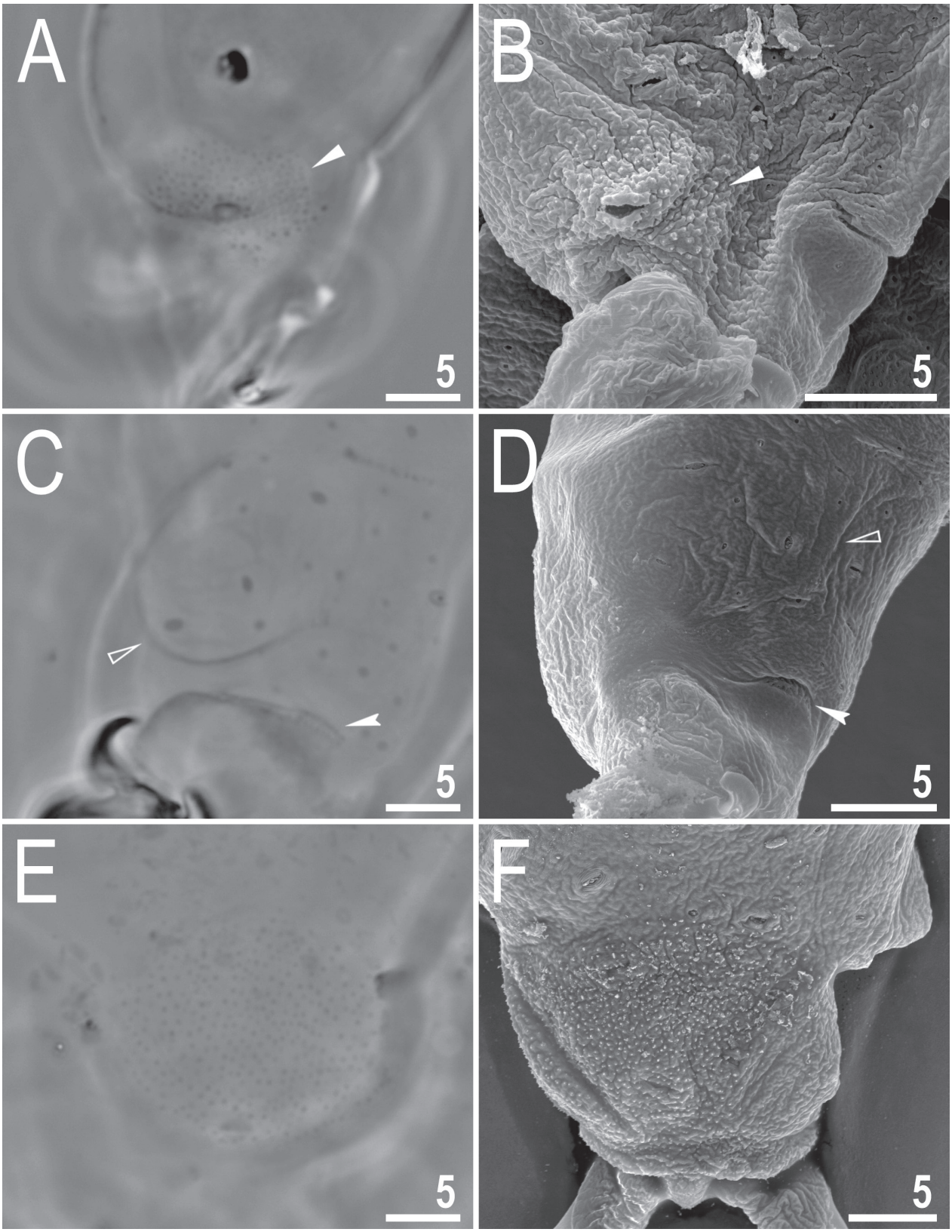

Figure 10. *Macrobiotus rybaki* sp. nov. – cuticular structures on legs: **A, B.** External granulation on leg III and II under PCM and SEM, respectively; **C, D.** A cuticular bulge (pulvinus) on the internal surface of legs III under PCM and SEM, respectively; **E, F.** Granulation on legs IV under PCM and SEM, respectively. Filled flat arrowheads indicate the granulation patch, empty flat arrowheads indicate pulvinus and filled indented arrowheads indicate muscle attachments. A and E assembled from several photos. Scale bars in μm.

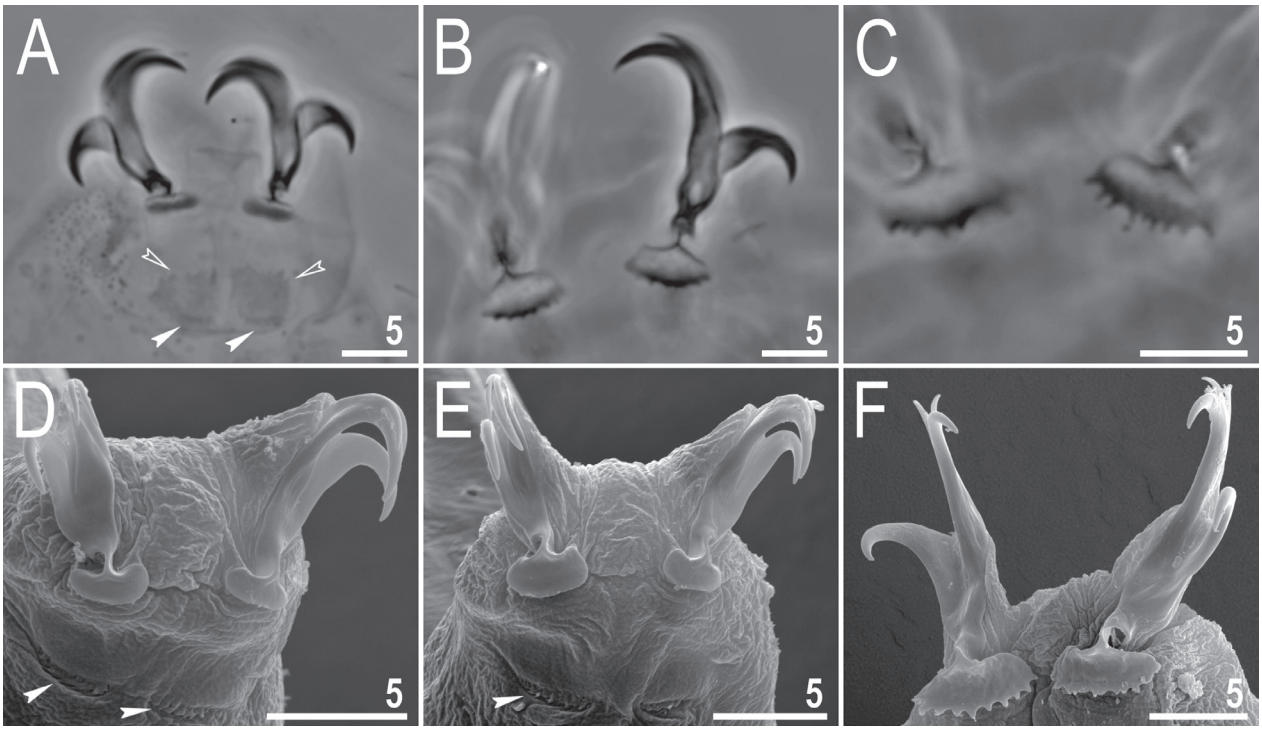

Figure 11. *Macrobiotus rybaki* sp. nov. – claws: **A, B.** Claws III and IV, respectively, under PCM; **C.** Magnification of lunulae IV of a different specimen; **D–F.** Claws II, III and IV respectively, under SEM. Filled indented arrowheads indicate double muscle attachments under the claws, empty indented arrowheads indicate a divided cuticular bar. **A** and **B** assembled from several photos. Scale bars in µm.

Processes are of the *hufelandi* type with very elongated concave trunk and extremely reduced (narrow), round and convex terminal discs with irregularly jagged edges (Figures 14C–F, 15). Under SEM the surface of the convex terminal discs is covered by small irregular granules and tubercles (Figures 15C–F).

Reproduction / Sexual dimorphism. The species is dioecious. Testis in males, which were clearly visible under PCM up to 24 hours after mounting in Hoyer's medium, have been found to be filled with spermatozoa, (Figure 16). In females spermathecae filled with spermatozoa were not observed. The species exhibits secondary sexual dimorphism in the form of small lateral gibbosities on the hind legs of males (Figure 16).

DNA sequences. 18S rRNA: GenBank: MW588028–MW588029; 1018 bp long.

28S rRNA: GenBank: MW588034–MW588035; 783 bp long.

ITS-2: GenBank: MW588022–MW588023; 391 bp long.

COI: GenBank: MW593931–MW593932; 658 bp long.

Phenotypic differential diagnosis. By having the OCA of the *patagonicus* type (only the 2nd and 3rd bands of teeth visible under light microscopy), egg chorion of the *hufelandi* type (covered with a reticulum), and egg processes with reduced (narrow) terminal disc, *Macrobiotus rybaki* sp. nov. is most similar to four species: *Macrobiotus dariae* Pilato & Bertolani, 2004, *Macrobiotus noemiae* Roszkowska & Kaczmarek, 2019, *Macrobiotus santoroi* Pilato & D'Urso, 1976 and *Macrobiotus serratus* Bertolani, Guidi & Rebecchi, 1996. The new species differs specifically from:

- ***M. dariae*** by having a more anteriorly placed stylet support insertion point (*pt 73–75.5* in the new species *vs. 77.2–77.9* in *M. dariae*), a narrower buccal tube external diameter (*pt 12.3–15.6* in the new species *vs. 15.6–25.7* in *M. dariae*), a smaller number of processes on the egg circumference (25–34 in the new species *vs.* 34–38 in *M. dariae*), a different egg process morphology (processes with very elongated concave trunks and extremely reduced – narrow – convex terminal discs in the new species *vs.* conical processes with flexible distal portion without terminal discs in *M. dariae*; Figure 18A–C).
- ***M. noemiae*** by having a more anterior stylet support insertion point (*pt 73.0–75.5* in the new species *vs. 78.3–81.8* in *M. noemiae*), by a smaller number of processes on the egg circumference (25–34 in the new species *vs.* 35–36 in *M. noemiae*), by well-defined reticulation on the chorion surface with the peribasal mesh larger than the interbasal mesh and mesh diameter larger than the walls and nodes of the reticulum (very delicate and faint reticulation with mesh of uniform size distributed randomly on the

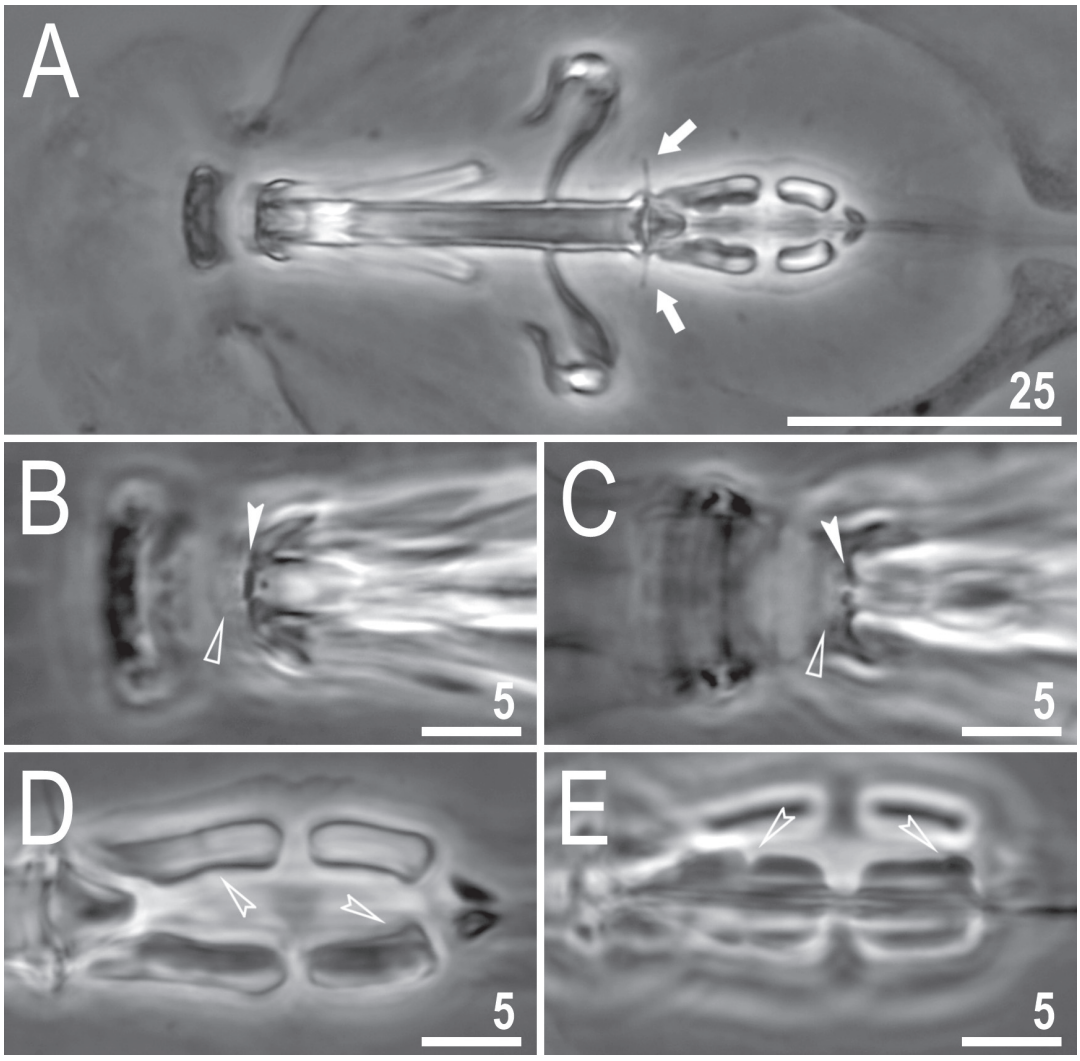

Figure 12. *Macrobiotus rybaki* sp. nov. – buccal apparatus and the oral cavity armature under PCM: **A.** Dorso-ventral view of the entire buccal apparatus; **B, C.** Oral cavity armature in dorsal and ventral view, respectively; **D, E.** Placoid morphology in dorsal and ventral view, respectively. Empty flat arrowheads indicate the second band of teeth, filled indented arrowheads indicate the third band of teeth in the oral cavity, empty indented arrowheads indicate central constriction in the first macroplacoid and subterminal constriction in the second macroplacoid and arrows indicate cuticular spikes between end of the buccal tube and anterior portion of the bulbus. **A, D, E** assembled from several photos. Scale bars in μm.

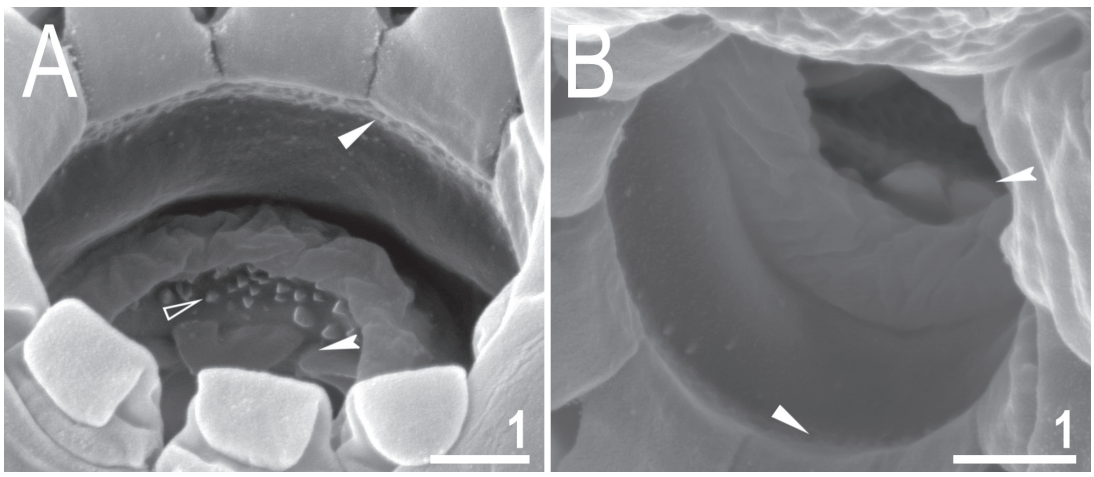

Figure 13. *Macrobiotus rybaki* sp. nov. – anterior view of the oral cavity armature under SEM: **A, B.** Dorsal and ventral view, respectively. Filled flat arrowheads indicate the first band of teeth, empty flat arrowhead indicates the second band of teeth, filled indented arrowheads indicate the third band of teeth in the oral cavity. Scale bars in μm.

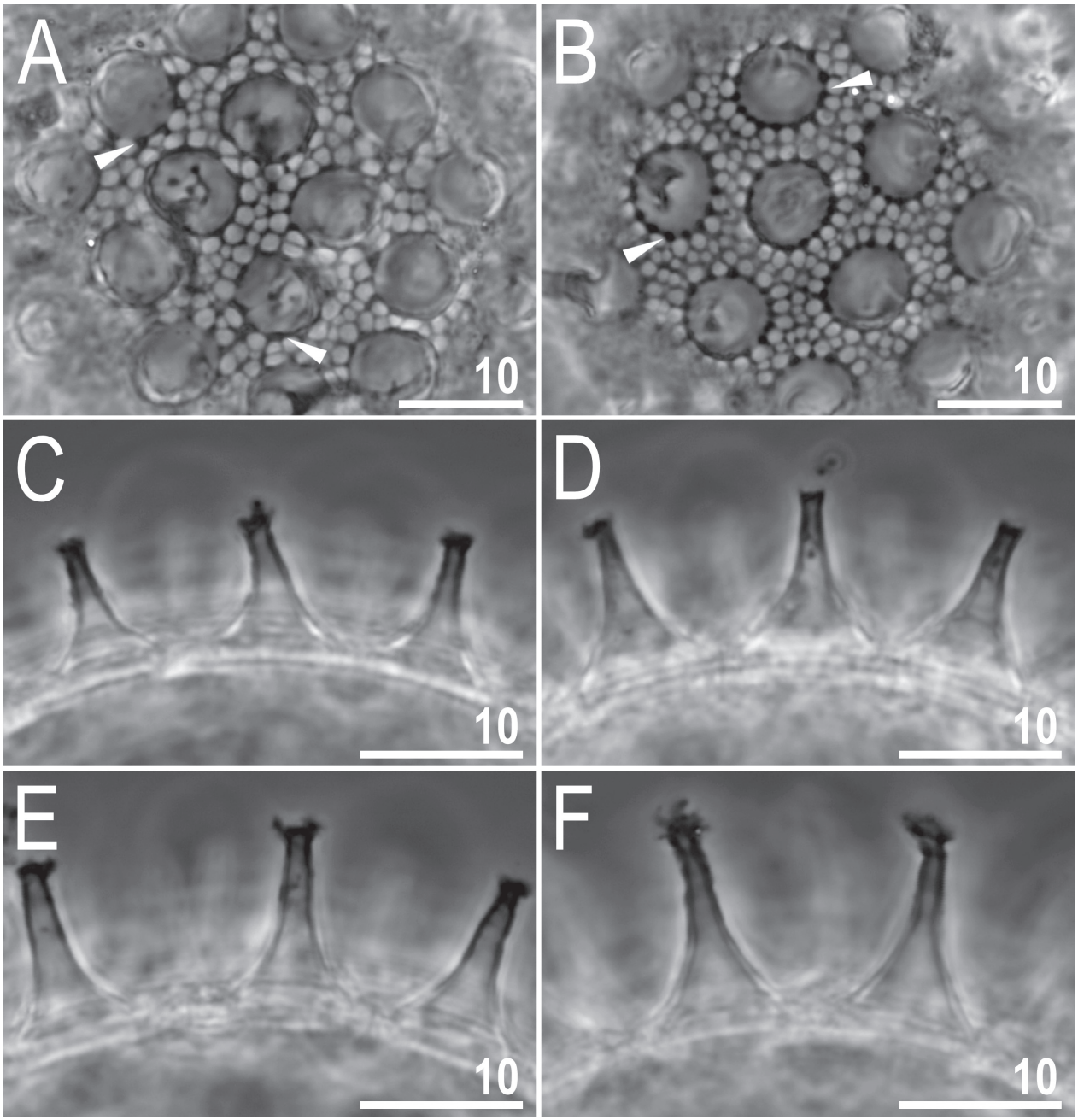

Figure 14. *Macrobiotus rybaki* sp. nov. – egg chorion morphology under PCM: **A, B.** Egg surface; **C–F.** Midsection of the processes. Filled flat arrowheads indicate cuticular thickenings around the processes base that merge into the bars and nodes of the reticulum. Scale bars in µm.

egg surface between the processes in *M. noemiae*), a different egg processes morphology (processes with very elongated concave trunks and extremely reduced – narrow – convex terminal discs without flexible filaments in the new species *vs.* conical processes without terminal discs but with hair-like, and flexible filaments in *M. noemiae*).

- ***M. santoroi*** by having taller egg processes (6.7–13.4 µm in the new species *vs.* 4 µm or less in *M. santoroi*), by a smaller number of processes on the egg circumference (25–34 in the new species *vs.* 37–40 in *M. santoroi*), by processes with very elongated concave trunks (processes peg-shaped in *M. santoroi*), by well-defined reticulation on the chorion surface with the peribasal mesh larger than the interbasal mesh and mesh diameter larger than walls and nodes of the reticulum (very fine mesh with evident and wide walls and nodes, giving the false impression of a granulated surface in *M. santoroi*).
- ***M. serratus*** by having a more anterior stylet support insertion (*pt 73.0–75.5* in the new species *vs. 75.6–77.7* in *M. serratus*), by a taller egg process height (6.7–13.4 µm in the new species *vs.* 5.5–6.0 µm in *M. serratus*) and by well-defined reticulation on the chorion surface with the peribasal mesh larger than the interbasal mesh and mesh diameter larger than

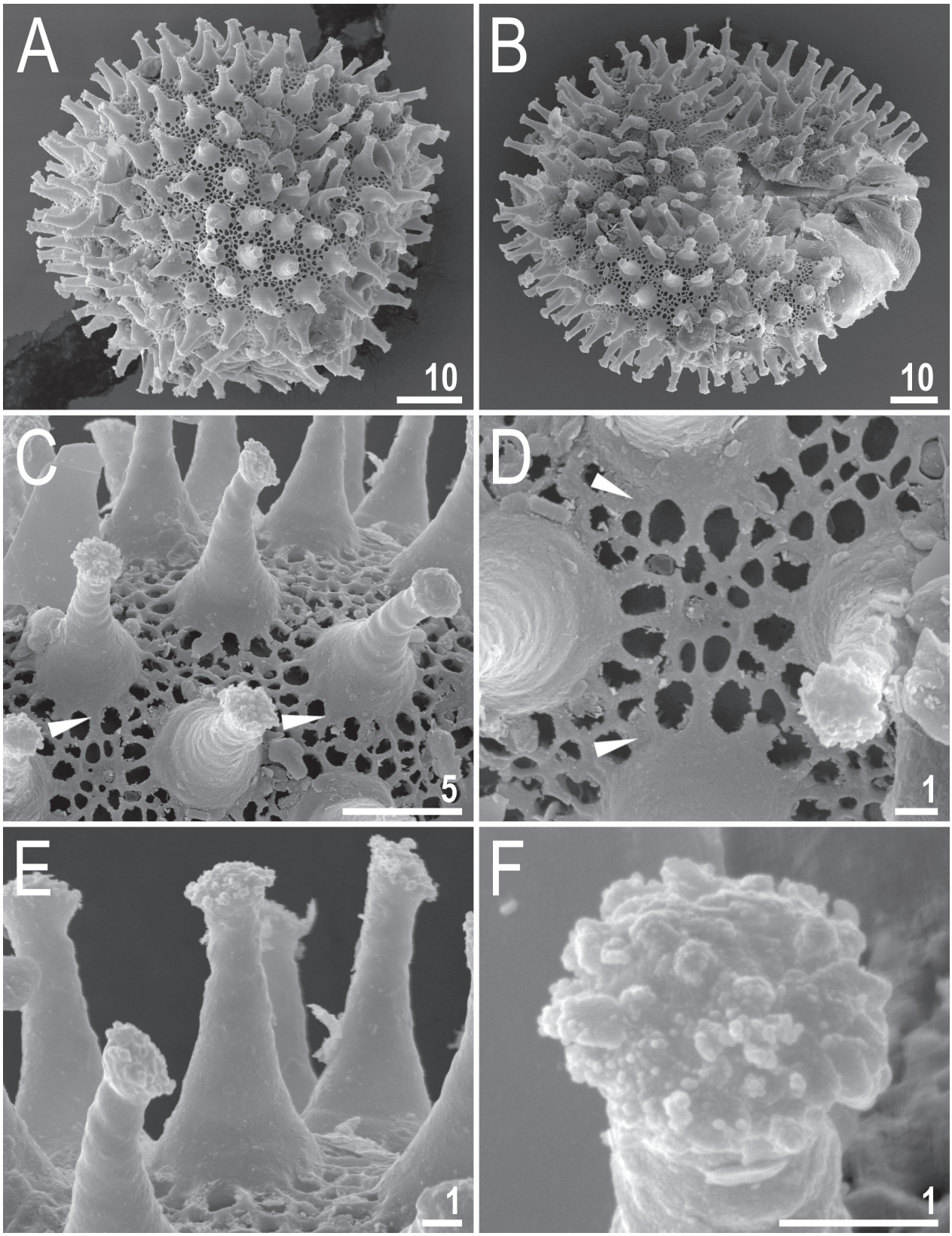

Figure 15. *Macrobiotus rybaki* sp. nov. – egg chorion morphology under SEM: **A, B.** Entire egg; **C–E.** Details of the egg processes and egg surface between them; **F.** Details of the reduced terminal disc. Filled flat arrowheads indicate cuticular thickenings around the processes base that merge into the bars and nodes of the reticulum. Scale bars in μm.

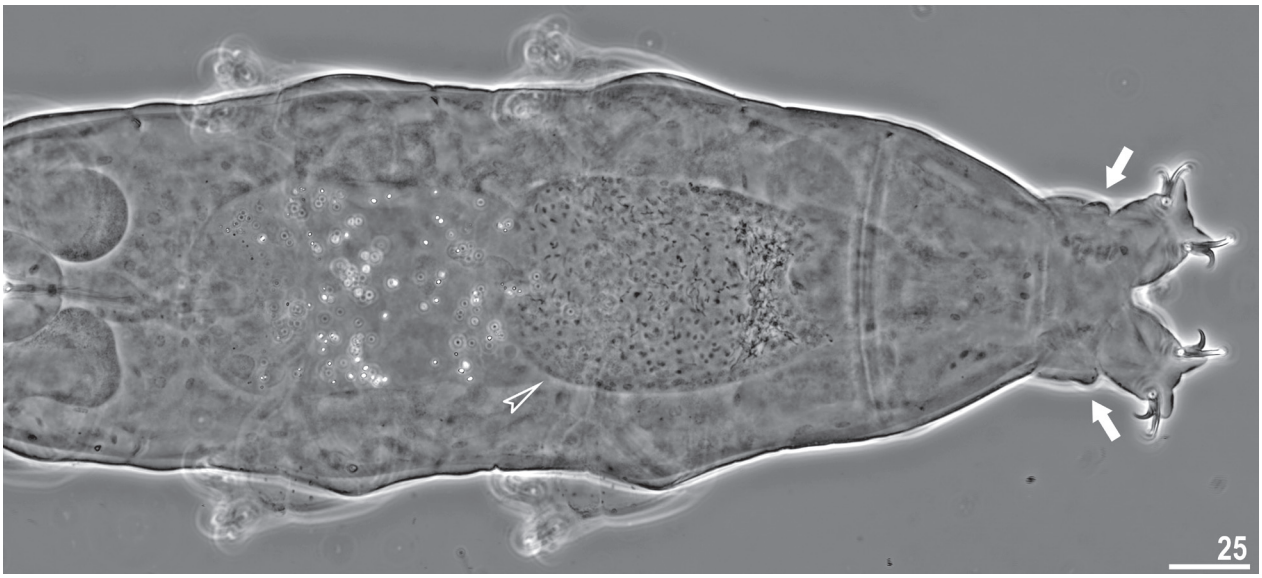

Figure 16. *Macrobiotus rybaki* sp. nov. – reproduction: male under PCM. Empty indented arrowhead indicates male's testis and arrows indicate lateral gibbosities on legs IV. Scale bar in µm.

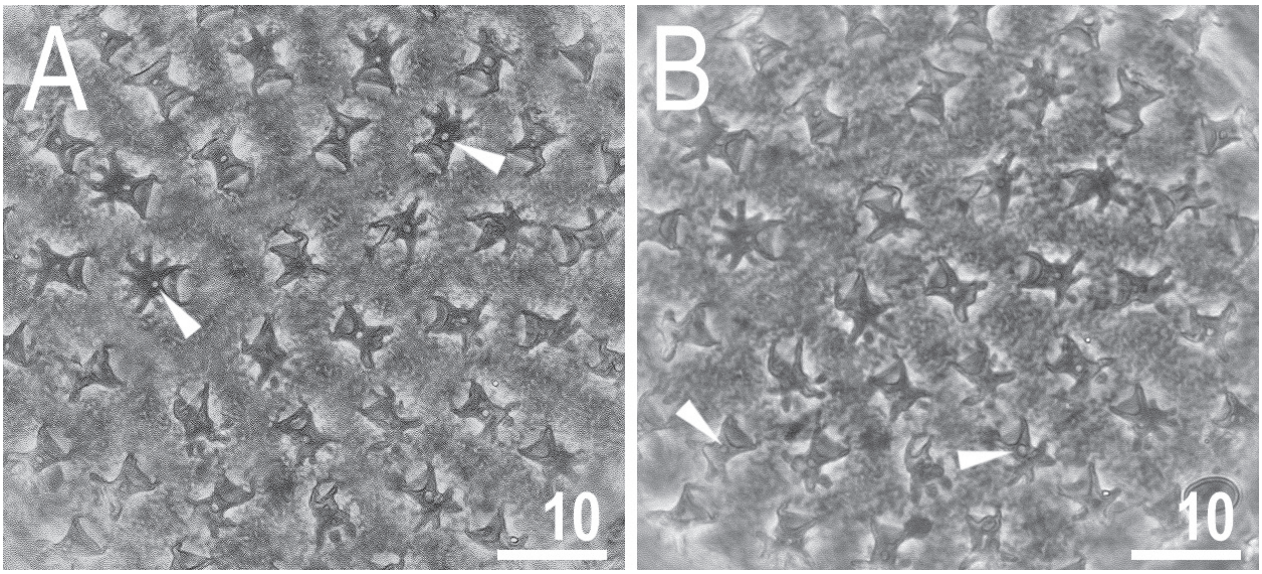

Figure 17. *Macrobiotus anemone* Meyer, Domingue & Hinton, 2014 (type series) – egg chorion morphology under PCM: **A, B.** Egg surface (slides 9551 and 9552 respectively). Filled flat arrowheads indicate a cavity between the process trunk and tentacular arms that appears in PCM as a clearly refracted dot. Scale bars in µm.

walls and nodes of the reticulum (very delicate and faint reticulation with mesh of similar sizes distributed uniformly on the egg surface between processes in *M. serratus*; Figure 18D, E).

Phylogenetic analysis. The phylogenetic reconstruction (Figure 19) recovered the genus *Macrobiotus* as well as the three clades found by Stec et al. (2021) and by Kiosya et al. (2021) to be monophyletic. All three clades have high support values (pp=1). The new species *Macrobiotus annewintersae* sp. nov. belongs to subclade B, within the *Macrobiotus persimilis* complex, even though the monophyly of this complex was not strongly supported (pp=0.73). *Macrobiotus engbergi* Stec, Tumanov & Kristensen, 2020 was recovered as the closest relative of *M. annewintersae* sp. nov. (Figure 19). The second species analysed in this study, *Macrobiotus rybaki* sp. nov., belongs to subclade A with its closest relatives being *Macrobiotus wandae* Kayastha, Berdi, Miaduchowska, Gawlak, Łukasiewicz, Gołdyn & Kaczmarek, 2020 and *Macrobiotus vladimiri* Bertolani, Biserov, Rebecchi & Cesari, 2011 (Figure 19). The newly found Swedish population identified in this study as *Macrobiotus* aff. *polonicus*, as could have been predicted from its morphological similarity with that species, clusters together with two populations of *Macrobiotus polonicus* Pilato, Kaczmarek, Michalczyk & Lisi, 2003 from Austria and Slovakia (Figure 19).

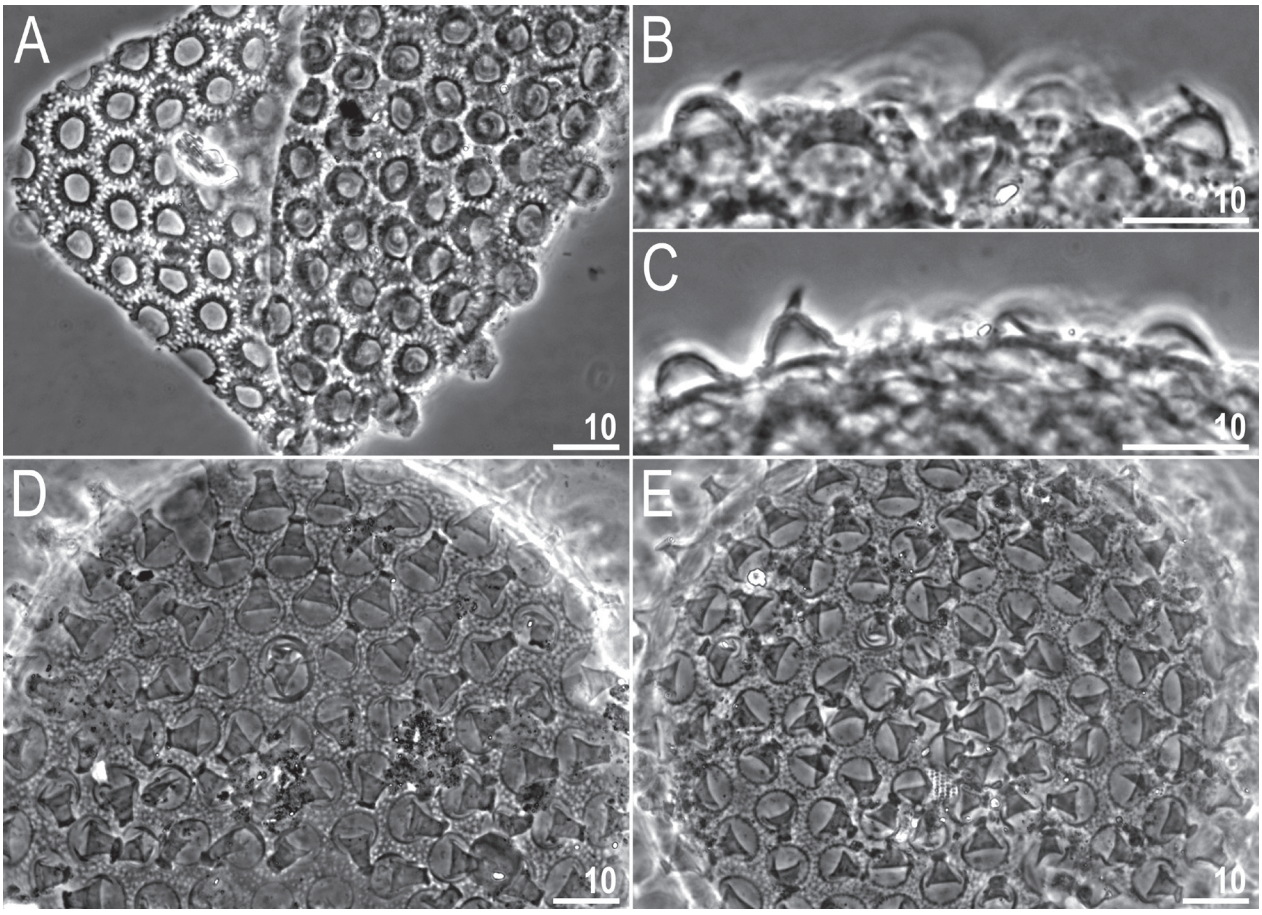

Figure 18. *Macrobiotus dariae* Pilato & Bertolani, 2004 and *Macrobiotus serratus* Bertolani, Guidi & Rebecchi, 1996 (type series) – egg chorion morphology under PCM: **A–C.** Egg surface (**A**) and midsections of the processes (**B, C**) of *M. dariae* (slides PC45s1 and PC45s3 respectively); **D, E.** Egg surface of *M. serratus* (slides C1907s17 and C1907s30 respectively). Scale bars in µm.

Discussion

We identified two new tardigrade species in the genus *Macrobiotus* using an integrative taxonomy approach combining the analyses of detailed morphological and genetic data. Thanks to the phylogenetic analysis performed in this study we confirmed *Macrobiotus annewintersae* sp. nov. to belong to the *Macrobiotus persimilis* complex (as defined by Stec et al. 2021). Nevertheless, the morphological definition provided by Stec et al. (2021) does not encompass the extraordinary egg phenotype exhibited by *Macrobiotus annewintersae* sp. nov., indicating the need for further amendment of the characters describing this monophyletic group of species. The definition of that complex, regarding the egg processes, states "[…] single-walled egg processes […] in the shape of truncated cones terminated with a well-developed disc and with solid chorion surface […]", It is therefore clear that as *M. annewintersae* sp. nov. possesses 2–8 tentacular arms on the distal part of its egg processes, as opposed to 'well-developed discs', it falls outside the current definition of the group. Very similar egg processes are also present in *M. anemone*, which was previously included in the *M. persimilis* complex by Stec et al. (2021) without any elaboration on that issue (please see Table 5 in Stec et al. (2021) for the list of species included there in the complex). Therefore, to avoid inconsistency in accommodating these two species within the *M. persimilis* complex, we propose an upgraded definition that reads: species with white body, *hufelandi* type claws and with single-walled egg processes (without the labyrinthine layer = not reticulated) in the shape of truncated cones terminated with a well-developed disc or tentacular arms and with a solid chorion surface (the surface can be wrinkled and sometimes with faintly visible micropores but never properly porous or reticulated). Furthermore, we propose to tentatively include *Macrobiotus andinus* Maucci, 1988 within the *M. persimilis* complex. The species meet now all the criteria except the porous cuticle, (hence it was not considered as a member of the *hufelandi* group *sensu* Kaczmarek and Michalczyk (2017), but it is likely that these pores could be visible only under SEM similarly as in same species of the *Macrobiotus pseudohufelandi* complex (Stec et al. 2021).

In their faunistic study devoted to Greek tardigrades Maucci and Durante Pasa (1982) reported *Macrobiotus anderssoni* Richters, 1907, specifically from the island of Crete. According to the description provided by Maucci and Durante Pasa (1982), their *Macrobiotus anderssoni* population from Crete is very similar to *M. rybaki* sp.

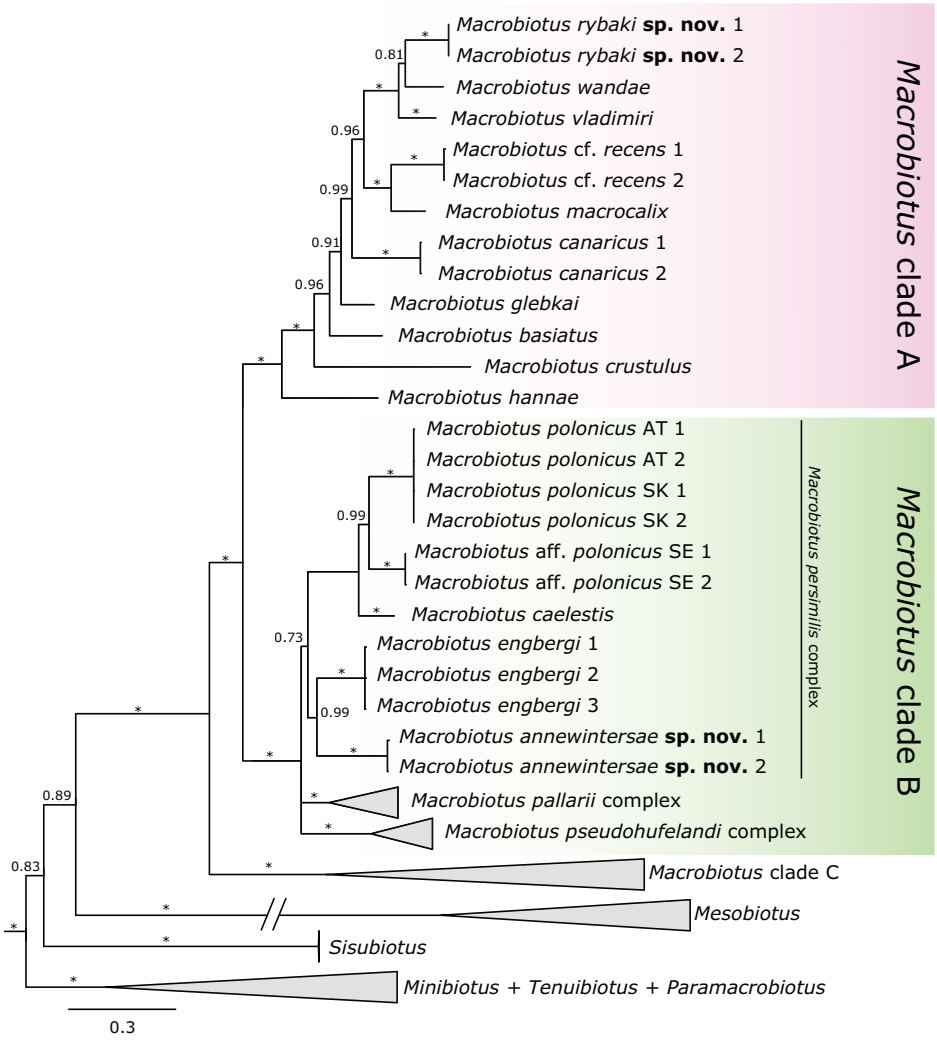

Figure 19. Phylogenetic reconstruction of the genus *Macrobiotus*, topology of BI analysis. Nodes with pp<70 were collapsed. Clades A–C from Stec et al. (2021) are indicated. * indicates nodes with support pp=1. Numbers after species names (when present) indicate different haplotypes or individuals from the same population. Outgroups not shown. Country abbreviations after species names (when present) indicate different populations (AT: Austria; SE: Sweden; SK: Slovakia).

nov. described in our study, with the only considerable difference being dentation on lunulae IV, that is present only in *M. rybaki* sp. nov.. Therefore, it is highly likely that these two populations represent closely related taxa, however, more populations from this region should be examined using an integrative approach to reliably test such a hypothesis.

Based on newly found *M. anderssoni* material, Maucci and Durante Pasa (1982) proposed a redescription of that species. However, the proposed redescription cannot be considered as valid as they failed to designate a neotype. Even if they had done so, several regulations of the International Code of Zoological Nomenclature (ICZN 1999) and the conditions listed in Article 75.3 of the code would not have been fulfilled. Specifically, (*i*) the authors did not provide reasons for believing the name-bearing type specimen(s) (i.e., holotype, or lectotype, or all syntypes, or prior neotype) to be lost or destroyed, and the steps that had been taken to trace it or them; (*ii*) the population that they studied did not come, as nearly as practicable, from the original type locality (terra typica of *M. anderssoni* is Tierra del Fuego in Argentina). Moreover, Roszkowska et al. (2016) have already questioned the identification of the population from Crete, stating that it belongs to an unrecognised species of the *Macrobiotus hufelandi* group. In light of the discussion in Roszkowska et al. (2016) on the taxonomic uncertainty concerning *M. anderssoni*, further supported by the newly found egg that fits perfectly with Richters' description and which was found near *terra typica*, we agree with the authors' claims that it is highly likely that *M. anderssoni* represents the genus *Mesobiotus* Vecchi, Cesari, Bertolani, Jönsson, Rebecchi & Guidetti, 2016. Nevertheless, a more robust conclusion can only be made following an integrative redescription of the species, based on a population from Tierra del Fuego or nearby locality, becoming available.

Our study describes yet another two new species of the genus *Macrobiotus* utilising the integrative taxonomy approach. The detailed morphological examination linked with genetic data in the form of DNA sequences

has allowed us also to elucidate the phylogenetic position of the studied taxa and amend the definition of the *Macrobiotus persimilis* complex. This further underlines the pre-eminence of the integrative approach, compared with classical taxonomy, in more reliably testing species hypotheses.

Acknowledgements

We are especially grateful to our colleagues Anne Winters, Małgorzata Mitan and Małgorzata Osielczak for collecting samples which enabled us to conduct this study and to Brian Blagden as well as Łukasz Michalczyk and Sara Calhim for improving the English and their critical reading of our manuscript. Moreover, we thank Roberto Guidetti, Roberto Bertolani, Witold Morek, Piotr Gąsiorek and the Natural History Museum of Verona for making the Bertolani and Maucci collections available and providing photographs of *M. dariae*, *M. serratus* and *M. andinus* type material and Harry Meyer for providing photographs of *M. anemone* type material. We also thank Edoardo Massa, Yevgen Kiosya and an anonymous reviewer for their constructive criticism. During this study, DS was a beneficiary of a National Science Centre scholarship to support doctoral research (no. 2019/32/T/NZ8/00348) and MV was supported by the Academy of Finland (Fellowship #314219 to Sara Calhim). The study was supported by the *Sonata Bis* programme of the Polish National Science Centre (grant no. 2016/22/E/NZ8/00417 to Łukasz Michalczyk) and by the Academy of Finland Fellowship to Sara Calhim (#314219).

References

Astrin JJ, Stüben PE (2008) Phylogeny in cryptic weevils: molecules, morphology and new genera of western Palaearctic Cryptorhynchinae (Coleoptera: Curculionidae). Invertebrate Systematics 22(5): 503–522. https://doi.org/10.1071/IS07057

Bah T (2011) Inkscape: guide to a vector drawing program (Vol. 559). Upper Saddle River, NJ, USA: Prentice Hall.

Bartels PJ, Nelson DR (2007) An evaluation of species richness estimators for tardigrades of the Great Smoky Mountains National Park, Tennessee and North Carolina, USA. Journal of Limnology 66: e104. https://doi.org/10.4081/jlimnol.2007.s1.104

Bartels PJ, Nelson DR, Exline RP (2011) Allometry and the removal of body size effects in the morphometric analysis of tardigrades. Journal of Zoological Systematics and Evolutionary Research 49: 17–25. https://doi.org/10.1111/j.1439-0469.2010.00593.x

Bertolani R (1982) A new genus and five new species of Italian fresh-water tardigrades. Bollettino del Museo Civico di storia Naturale, Verona 114: 249–254.

Bertolani R, Guidi A, Rebecchi L (1996) Tardigradi della Sardegna e di alcune piccole isole circumsarde. Biogeographia – The Journal of Integrative Biogeography 18(1): 229–247. https://doi.org/10.21426/B618110456

Bertolani R, Biserov V, Rebecchi L, Cesari M (2011) Taxonomy and biogeography of tardigrades using an integrated approach: new results on species of the *Macrobiotus hufelandi* group. Invertebrate Zoology 8(1): 23–36. https://doi.org/10.15298/invertzool.08.1.05

Bertolani R, Guidetti R, Marchioro T, Altiero T, Rebecchi L, Cesari M (2014) Phylogeny of Eutardigrada: New molecular data and their morphological support lead to the identification of new evolutionary lineages. Molecular Phylogenetics and Evolution 76: 110–126. https://doi.org/10.1016/j.ympev.2014.03.006

Bochnak M, Vončina K, Kristensen RM, Gąsiorek P (2020) Continued exploration of Tanzanian rainforests reveals a new echiniscid species (Heterotardigrada). Zoological Studies 59(18): 1–13. https://doi.org/10.6620/ZS.2020.59-18

Casquet J, Thebaud C, Gillespie RG (2012) Chelex without boiling, a rapid and easy technique to obtain stable amplifiable DNA from small amounts of ethanol-stored spiders. Molecular Ecology Resources 12: 136–141. https://doi.org/10.1111/j.1755-0998.2011.03073.x

Coughlan K, Stec D (2019) Two new species of the *Macrobiotus hufelandi* complex (Tardigrada: Eutardigrada: Macrobiotidae) from Australia and India, with notes on their phylogenetic position. European Journal of Taxonomy 573: 1–38. https://doi.org/10.5852/ejt.2019.573

Coughlan K, Michalczyk Ł, Stec D (2019) *Macrobiotus caelestis* sp. nov., a new tardigrade species (Macrobiotidae: *hufelandi* group) from the Tien Shan mountains (Kyrgyzstan). Annales Zoologici 69(3): 499–513. https://doi.org/10.3161/00034541ANZ2019.69.3.002

Dastych H (1980) Niesporczaki (Tardigrada) Tatrzańskiego Parku Narodowego. Monografie Fauny Polski 9: 1–232.

Degma P, Guidetti R (2007) Notes to the current checklist of Tardigrada. Zootaxa 1579: 41–53. https://doi.org/10.11646/zootaxa.1579.1.2

Degma P, Bertolani R, Guidetti R (2020) Actual checklist of Tardigrada species (2009–2020, 39th edn.). [Accessed 20 January 2021.] https://doi.org/10.25431/11380_1178608.

Doyère ML (1840) Memorie sur les Tardigrades. Annales des Sciences Naturelles. Zoologie 14: 269–362.

Durante Pasa MV, Maucci W (1979) Tardigradi muscicoli della Grecia. Zeszyty Naukowe Uniwersytetu Jagiellohskiego 529: 19–45.

Edgar R (2004) MUSCLE: multiple sequence alignment with high accuracy and high throughput. Nucleic Acids Research 32(5): 1792–1797. https://doi.org/10.1093/nar/gkh340

Gąsiorek P, Stec D, Zawierucha Z, Kristensen RM, Michalczyk Ł (2018) Revision of *Testechiniscus* Kristensen, 1987 (Heterotardigrada: Echiniscidae) refutes the polar-temperate distribution of the genus. Zootaxa 4472(2): 261–297. https://doi.org/10.11646/zootaxa.4472.2.3

Guidetti R, Bertolani R (2005) Tardigrade taxonomy: an updated check list of the taxa and a list of characters for their identification. Zootaxa 845: 1–46. https://doi.org/10.11646/zootaxa.845.1.1

Guidetti R, Schill RO, Giovannini I, Massa E, Goldoni SE, Ebel C, Förschler MI, Rebecchi L, Cesari M (2021) When DNA sequence data and morphological results fit together: Phylogenetic position of *Crenubiotus* within Macrobiotoidea (Eutardigrada) with description of *Crenubiotus ruhesteini* sp. nov. Journal of Zoological Systematics and Evolutionary Research 59(3): 576–587. https://doi.org/10.1111/jzs.12449

Hinton JG, Meyer HA (2009) Tardigrada of Mississippi. Proceedings of the Louisiana Academy of Sciences 67: 23–27.

ICZN (1999) International code of zoological nomenclature. International Trust for Zoological Nomenclature. https://www.iczn.org/the-code/the-international-code-of-zoological-nomenclature/the-code-online/

Kaczmarek Ł, Michalczyk Ł (2017) The *Macrobiotus hufelandi* group (Tardigrada) revisited. Zootaxa 4363(1): 101–123. https://doi.org/10.11646/zootaxa.4363.1.4

Kaczmarek Ł, Cytan J, Zawierucha K, Diduszko D, Michalczyk Ł (2014) Tardigrades from Peru (South America), with descriptions of three new species of Parachela. Zootaxa 3790(2): 357–379. https://doi.org/10.11646/zootaxa.3790.2.5

Kaczmarek Ł, Michalczyk Ł, McInnes SJ (2016) Annotated zoogeography of non-marine Tardigrada. Part III: North America and Greenland. Zootaxa 4203(1): 1–249. https://doi.org/10.11646/zootaxa.4203.1.1

Kaczmarek Ł, Zawierucha K, Buda J, Stec D, Gawlak M, Michalczyk Ł, Roszkowska M (2018) An integrative redescription of the nominal taxon for the *Mesobiotus harmsworthi* group (Tardigrada: Macrobiotidae) leads to descriptions of two new *Mesobiotus* species from Arctic. PLoS ONE 13(10): e0204756. https://doi.org/10.1371/journal.pone.0204756

Katoh K, Toh H (2008) Recent developments in the MAFFT multiple sequence alignment program. Brief Bioinformatics 9: 286–298. https://doi.org/10.1093/bib/bbn013

Katoh K, Misawa K, Kuma K, Miyata T (2002) MAFFT: A novel method for rapid multiple sequence alignment based on fast Fourier transform. Nucleic Acids Resources 30: 3059–3066. https://doi.org/10.1093/nar/gkf436

Kayastha P, Berdi D, Mioduchowska M, Gawlak M, Łukasiewicz A, Gołdyn B, Kaczmarek Ł (2020a) Some tardigrades from Nepal (Asia) with integrative description of *Macrobiotus wandae* sp. nov. (Macrobiotidae: *hufelandi* group). Annales Zoologici 70(1): 121–142. https://doi.org/10.3161/00034541ANZ2020.70.1.007

Kayastha P, Bartylak T, Gawlak M, Kaczmarek Ł (2020b) Integrative Description of *Pseudechiniscus lalitae* sp. nov. (Tardigrada: Heterotardigrada: Echiniscidae) from the Azores Archipelago (Portugal). Annales Zoologici 70(4): 487–505. https://doi.org/10.3161/00034541ANZ2020.70.4.002

Kiosya Y, Pogwizd J, Matsko Y, Vecchi M, Stec D (2021) Phylogenetic position of two *Macrobiotus* species with a revisional note on *Macrobiotus sottilei* Pilato, Kiosya, Lisi and Sabella, 2012 (Tardigrada: Eutardigrada: Macrobiotidae). Zootaxa 49333(1): 113–135. https://doi.org/10.11646/zootaxa.4933.1.5

Kumar S, Stecher G, Tamura K (2016) MEGA7: Molecular Evolutionary Genetics Analysis version 7.0 for bigger datasets. Molecular Biology and Evolution 33: 1870–1874. https://doi.org/10.1093/molbev/msw054

Kuzdrowska K, Mioduchowska M, Gawlak M, Barylak T, Kepel A, Kepel M, Kaczmarek Ł (2021) Integrative description of *Macrobiotus porifini* sp. nov. (Macrobiotidae) from Madagascar and its phylogenetic position within the *hufelandi* group. European Zoological Journal 88(1): 375–389. https://doi.org/10.1080/24750263.2021.1883752

Lanfear R, Frandsen PB, Wright AM, Senfeld T, Calcott B (2016) PartitionFinder 2: new methods for selecting partitioned models of evolution for molecular and morphological phylogenetic analyses. Molecular Biology and Evolution 34: 772–773. https://doi.org/10.1093/molbev/msw260

Maucci W (1988) Tardigrada from Patagonia (Southern South America) with description of three new species. Revista Chilena de Entomología 16: 5–13.

Maucci W, Durante Pasa MV (1982) Tardigradi della Grecia (secondo contributo), con particolare riferimento alla fauna del'isola di Creta. Bollettino del Museo Civico di Storia Naturale di Verona 9: 479–488.

Marcus E (1936) Tardigrada. Das Tierreich 66, 340 pp.

Marley NJ, McInnes SJ, Sands CJ (2011) Phylum Tardigrada: a re-evaluation of the Parachela. Zootaxa 2819: 51–64. https://doi.org/10.11646/zootaxa.2819.1.2

Meyer HA (2013) Terrestrial and freshwater Tardigrada of the Americas. Zootaxa 3747(1): 1–71. https://doi.org/10.11646/zootaxa.3747.1.1

Meyer HA, Domingue MN, Hinton JG (2014) Tardigrada of the West Gulf Coastal Plain, with descriptions of two new species from Louisiana. Southeastern Naturalist 13(5): 117–130. https://doi.org/10.11646/zootaxa.3747.1.1

Michalczyk Ł, Kaczmarek Ł (2003) A description of the new tardigrade *Macrobiotus reinhardti* (Eutardigrada: Macrobiotidae, *harmsworthi* group) with some remarks on the oral cavity armature within the genus *Macrobiotus* Schultze. Zootaxa 331(1): 1–24. https://doi.org/10.11646/zootaxa.331.1.1

Michalczyk Ł, Kaczmarek Ł (2013) The Tardigrada Register: a comprehensive online data repository for tardigrade taxonomy. Journal of Limnology 72(s1): 175–181. https://doi.org/10.4081/jlimnol.2013.s1.e22

Miller MA, Pfeiffer W, Schwartz T (2010) Creating the CIPRES Science Gateway for inference of large phylogenetic trees. 2010 gateway computing environments workshop (GCE): 1–8. https://doi.org/10.1109/GCE.2010.5676129

Mironov SV, Dabert J, Dabert M (2012) A new feather mite species of the genus *Proctophyllodes* Robin, 1877 (Astigmata: Proctophyllodidae) from the Long-tailed Tit *Aegithalos caudatus* (Passeriformes: Aegithalidae): morphological description with DNA barcode data. Zootaxa 3253: 54–61. https://doi.org/10.11646/zootaxa.3253.1.2

Morek W, Stec D, Gąsiorek P, Schill RO, Kaczmarek Ł, Michalczyk Ł (2016) An experimental test of eutardigrade preparation methods for light microscopy. Zoological Journal of the Linnean Society 178: 785–793. https://doi.org/10.1111/zoj.12457

Morek W, Ciosek JA, Michalczyk Ł (2020) Description of *Milnesium pentapapillatum* sp. nov., with an amendment of the diagnosis of the order Apochela and abolition of the class Apotardigrada (Tardigrada). Zoologischer Anzeiger 288: 107–117. https://doi.org/10.1016/j.jcz.2020.07.002

Nelson DR, Fletcher RA, Guidetti R, Roszkowska M, Grobys D, Kaczmarek Ł (2020a) Two new species of Tardigrada from moss cushions (*Grimmia* sp.) in a xerothermic habitat in northeast Tennessee (USA, North America), with the first identification of males in the genus *Viridiscus*. PeerJ 8: e10251. https://doi.org/10.7717/peerj.10251

Nelson DR, Bartels PJ, Fegley SR (2020b) Environmental correlates of tardigrade community structure in mosses and lichens in the Great Smoky Mountains National Park (Tennessee and North Carolina, USA). Zoological Journal of the Linnean Society 188(3): 913–924. https://doi.org/10.1093/zoolinnean/zlz043

Nowak B, Stec D (2018) An integrative description of *Macrobiotus hannae* sp. nov. (Tardigrada: Eutardigrada: Macrobiotidae: *hufelandi* group) from Poland. Turkish Journal of Zoology 42(3): 269–286. https://doi.org/10.3906/zoo-1712-31

Pilato G (1981) Analisi di nuovi caratteri nello studio degli Eutardigradi. Animalia 8: 51–57.

Pilato G, D'Urso V (1976) Contributo alla conoscenza dei Tardigradi d'Australia. Animalia 3(1): 135–145.

Pilato G, Bertolani R (2004) *Macrobiotus dariae* sp. n., a new species of eutardigrade (Eutardigrada, Macrobiotidae) from Cyprus. Zootaxa 638(1): 1–7. https://doi.org/10.11646/zootaxa.638.1.1

Pilato G, Kaczmarek Ł, Michalczyk Ł, Lisi O (2003) *Macrobiotus polonicus*, a new species of Tardigrada from Poland (Eutardigrada: Macrobiotidae, '*hufelandi* group'). Zootaxa 258: 1–8. https://doi.org/10.11646/zootaxa.258.1.1

Pogwizd J, Stec D (2020) New records of *Dactylobiotus parthenogeneticus* Bertolani, 1982 provide insight into its genetic variability and geographic distribution. Folia Biologica 68(2): 57–72. https://doi.org/10.3409/fb_68-2.08

Rambaut A (2007) FigTree, a graphical viewer of phylogenetic trees.

Rambaut A, Drummond A, Xie D, Baele G, Suchard M (2018) Posterior Summarization in Bayesian Phylogenetics Using Tracer 1.7. Systematic Biology 67(5): 901–904. https://doi.org/10.1093/sysbio/syy032

R Core Team (2020) R: A language and environment for statistical computing. R Foundation for Statistical Computing, Vienna. https://www.R-project.org/

Richters F (1903) Nordische tardigraden. Zoologischer Anzeiger 27(5): 168–172.

Richters F (1907) Die Fauna der Moosrasen des Gaussbergush. IX. Tardigraden.

Richters F (1926) Tardigrada. In: Kükenthal W, Krumbach T (Eds) Handbuch der Zoologie 3: 58–61.

Ronquist F, Teslenko M, van der Mark P, Ayres D, Darling A, Höhna S, Larget B, Liu L, Suchard M, Huelsenbeck J (2012) MrBayes 3.2: Efficient Bayesian Phylogenetic Inference and Model Choice Across a Large Model Space. Systematic Biology 61(3): 539–542. https://doi.org/10.1093/sysbio/sys029

Roszkowska M, Kaczmarek Ł (2019) *Macrobiotus noemiae* sp. nov., a new tardigrade species (Macrobiotidae: *hufelandi* group) from Spain. Turkish Journal of Zoology 43(4): 331–348. https://doi.org/10.3906/zoo-1902-5

Roszkowska M, Stec D, Ciobanu DA, Kaczmarek Ł (2016) Tardigrades from Nahuel Huapi National Park (Argentina, South America) with descriptions of two new Macrobiotidae species. Zootaxa 4105(3): 243–260. https://doi.org/10.11646/zootaxa.4105.3.2

Roszkowska M, Ostrowska M, Stec D, Janko K, Kaczmarek Ł (2017) *Macrobiotus polypiformis* sp. nov., a new tardigrade (Macrobiotidae; *hufelandi* group) from the Ecuadorian Pacific coast, with remarks on the claw abnormalities in eutardigrades. European Journal of Taxonomy 327: 1–19. https://doi.org/10.5852/ejt.2017.327

Roszkowska M, Stec D, Gawlak M, Kaczmarek Ł (2018) An integrative description of a new tardigrade species *Mesobiotus romani* sp. nov. (Macrobiotidae: *harmsworthi* group) from the Ecuadorian Pacific coast. Zootaxa 4450(5): 550–564. https://doi.org/10.11646/zootaxa.4450.5.2

Schill RO (2019) Water bears: The biology of tardigrades (Vol. 2). Springer, 1409 pp. https://doi.org/10.1007/978-3-319-95702-9

Schultze CAS (1834) *Macrobiotus Hufelandii* animal e crustaceorum classe novum, reviviscendi post diuturnam asphixiam et aridiatem potens. C. Curths, Berlin, 6 pp.

Schuster RO, Nelson DR, Grigarick AA, Christenberry D (1980) Systematic criteria of the Eutardigrada. Transactions of the American Microscopical Society 99: 284–303. https://doi.org/10.2307/3226004

Stec D, Smolak R, Kaczmarek Ł, Michalczyk Ł (2015) An integrative description of *Macrobiotus paulinae* sp. nov. (Tardigrada: Eutardigrada: Macrobiotidae: *hufelandi* group) from Kenya. Zootaxa 4052: 501–526. https://doi.org/10.11646/zootaxa.4052.5.1

Stec D, Gąsiorek P, Morek W, Kosztyła P, Zawierucha K, Kaczmarek Ł, Prokop ZM, Michalczyk Ł (2016) Estimating optimal sample size for tardigrade morphometry. Zoological Journal of the Linnean Society 178: 776–784. https://doi.org/10.1111/zoj.12404

Stec D, Zawierucha K, Michalczyk Ł (2017a) An integrative description of *Ramazzottius subanomalus* (Biserov, 1985) (Tardigrada) from Poland. Zootaxa 4300(3): 403–420. https://doi.org/10.11646/zootaxa.4300.3.4

Stec D, Morek W, Gąsiorek P, Blagden B, Michalczyk Ł (2017b) Description of *Macrobiotus scoticus* sp. nov. (Tardigrada: Macrobiotidae: *hufelandi* group) from Scotland by means of integrative taxonomy. Annales Zoologici 67: 181–197. https://doi.org/10.3161/00034541ANZ2017.67.2.001

Stec D, Morek W, Gąsiorek P, Michalczyk Ł (2018a) Unmasking hidden species diversity within the *Ramazzottius oberhaeuseri* complex, with an integrative redescription of the nominal species for the family Ramazzottiidae (Tardigrada: Eutardigrada: Parachela). Systematics and Biodiversity 16(4): 357–376. https://doi.org/10.1080/14772000.2018.1424267

Stec D, Krzywański Ł, Michalczyk Ł (2018b) Integrative description of *Macrobiotus canaricus* sp. nov. with notes on *M. recens* (Eutardigrada: Macrobiotidae). European Journal of Taxonomy 452: 1–36. https://doi.org/10.5852/ejt.2018.452

Stec D, Kristensen RM, Michalczyk Ł (2018c) Integrative taxonomy identifies *Macrobiotus papei*, a new tardigrade species of the *Macrobiotus hufelandi* complex (Eutardigrada: Macrobiotidae) from the Udzungwa Mountains National Park (Tanzania). Zootaxa 4446(2): 273–291. https://doi.org/10.11646/zootaxa.4446.2.7

Stec D, Arakawa K, Michalczyk Ł (2018d) An integrative description of *Macrobiotus shonaicus* sp. nov. (Tardigrada: Macrobiotidae) from Japan with notes on its phylogenetic position within the *hufelandi* group. PLoS ONE 13(2): e0192210. https://doi.org/10.1371/journal.pone.0192210

Stec D, Roszkowska M, Kaczmarek L, Michalczyk Ł (2018e) An integrative description of a population of *Mesobiotus radiatus* (Pilato, Binda and Catanzaro, 1991) from Kenya. Turkish Journal of Zoology 42(5): 523–540. https://doi.org/10.3906/zoo-1802-43

Stec D, Roszkowska M, Kaczmarek Ł, Michalczyk Ł (2018f) *Paramacrobiotus lachowskae*, a new species of Tardigrada from Colombia (Eutardigrada: Parachela: Macrobiotidae). New Zealand Journal of Zoology 45(1): 43–60. https://doi.org/10.1080/03014223.2017.1354896

Stec D, Kristensen RM, Michalczyk Ł (2020a) An integrative description of *Minibiotus ioculator* sp. nov. from the Republic of South Africa with notes on *Minibiotus pentannulatus* Londoño et al., 2017 (Tardigrada: Macrobiotidae). Zoologischer Anzeiger 286: 117–134. https://doi.org/10.1016/j.jcz.2020.03.007

Stec D, Tumanov DV, Kristensen RM (2020b) Integrative taxonomy identifies two new tardigrade species (Eutardigrada: Macrobiotidae) from Greenland. European Journal of Taxonomy 614: 1–40. https://doi.org/10.5852/ejt.2020.614

Stec D, Dudziak M, Michalczyk Ł (2020c) Integrative descriptions of two new Macrobiotidae species (Tardigrada: Eutardigrada: Macrobiotoidea) from French Guiana and Malaysian Borneo. Zoological Studies 59: 1–23. https://doi.org/10.6620/ZS.2020.59-23

Stec D, Krzywański Ł, Zawierucha K, Michalczyk Ł (2020d) Untangling systematics of the *Paramacrobiotus areolatus* species complex by an integrative redescription of the nominal species for the group, with multilocus phylogeny and species delineation in the genus *Paramacrobiotus*. Zoological Journal of the Linnean Society 188(3): 694–716. https://doi.org/10.1093/zoolinnean/zlz163

Stec D, Krzywański Ł, Arakawa K, Michalczyk Ł (2020e) A new redescription of *Richtersius coronifer*, supported by transcriptome, provides resources for describing concealed species diversity within the monotypic genus *Richtersius* (Eutardigrada). Zoological letters 6(1): 1–2. https://doi.org/10.1186/s40851-020-0154-y

Stec D, Vecchi M, Calhim S, Michalczyk Ł (2021) New multilocus phylogeny reorganises the family Macrobiotidae (Eutardigrada) and unveils complex morphological evolution of the *Macrobiotus hufelandi* group. Molecular Phylogenetics and Evolution 106987. https://doi.org/10.1016/j.ympev.2020.106987

Surmacz B, Morek W, Michalczyk Ł (2020) What to do when ontogenetic tracking is unavailable: a morphometric method to classify instars in *Milnesium* (Tardigrada). Zoological Journal of the Linnean Society 188(3): 797–808. https://doi.org/10.1093/zoolinnean/zlz099

Thulin G (1928) Über die Phylogenie und das System der Tardigraden. Hereditas 11: 207–266. https://doi.org/10.1111/j.1601-5223.1928.tb02488.x

Tumanov DV (2020a) Integrative redescription of *Hypsibius pallidoides* Pilato et al., 2011 (Eutardigrada: Hypsibioidea) with the erection of a new genus and discussion on the phylogeny of Hypsibiidae. European Journal of Taxonomy 681: 1–37. https://doi.org/10.5852/ejt.2020.681

Tumanov DV (2020b) Integrative description of *Mesobiotus anastasiae* sp. nov. (Eutardigrada, Macrobiotoidea) and first record of *Lobohalacarus* (Chelicerata, Trombidiformes) from the Republic of South Africa. European Journal of Taxonomy 726: 102–131. https://doi.org/10.11646/zootaxa.4450.5.2

Vecchi M, Cesari M, Bertolani R, Jönsson KI, Rebecchi L, Guidetti R (2016) Integrative systematic studies on tardigrades from Antarctica identify new genera and new species within Macrobiotoidea and Echiniscoidea. Invertebrate Systematics 30(4): 303–322. https://doi.org/10.1071/IS15033_CO

Vuori T, Massa E, Calhim S, Vecchi M (2020) Tardigrades of Finland: new records and an annotated checklist. Zootaxa 4851(3): 477–521. https://doi.org/10.11646/zootaxa.4851.3.3

Supplementary material 1

Raw morphometric data for *Macrobiotus annewintersae* sp. nov. from U.S.A (S207 – US.084, type population)

Authors: Matteo Vecchi, Daniel Stec
Data type: morphometric dataset

Link: https://doi.org/10.3897/zse.97.65280.suppl1

Supplementary material 2

Raw morphometric data for *Macrobiotus rybaki* sp. nov. from Greece (GR.011, type population)

Authors: Matteo Vecchi, Daniel Stec
Data type: morphometric dataset

Link: https://doi.org/10.3897/zse.97.65280.suppl2

Supplementary material 3

Thorpe normalization calculations and results

Authors: Matteo Vecchi, Daniel Stec
Data type: analysis raw results

Link: https://doi.org/10.3897/zse.97.65280.suppl3

Supplementary material 4

Partitions and models selection results

Authors: Matteo Vecchi, Daniel Stec
Data type: analysis raw results

Link: https://doi.org/10.3897/zse.97.65280.suppl4

Supplementary material 5

MrBayes analysis input file with the alignment

Authors: Matteo Vecchi, Daniel Stec
Data type: analysis input file

Link: https://doi.org/10.3897/zse.97.65280.suppl5

Supplementary material 6

MrBayes output consensus tree

Authors: Matteo Vecchi, Daniel Stec
Data type: analysis raw results

Link: https://doi.org/10.3897/zse.97.65280.suppl6